Doctoral Dissertation

Solvent Relaxation in Biomembranes: Application in the Development of Non-Viral Gene Transfection Carriers

Agnieszka Olżyńska

Supervised by Martin Hof

Department of Physical and Macromolecular Chemistry

Faculty of Science

Charles University

Prague, Czech Republic

Prague 2008

ABSTRACT

In order to study lipid membrane properties, fluorescence solvent relaxation method, which enables us to determine the degree of hydration of the membrane and the mobility of the hydrated lipid molecules, was used. Applying three different naphthalene derivatives as fluorescent dyes (Patman, Laurdan and Prodan) allowed probing different parts of the headgroup region of the bilayer. First, wavelength-dependent parallax quenching measurements resulted in the determination of precise locations of Laurdan and Patmant within the DOPC bilayer. Exploring the issue of the probes locations within the lipid bilayer, acrylamide quenching experiments were performed. They have shown Patman relocalization in cationic, DOTAP-containing systems. Bilayers formed from phosphatidylcholines with different alkyl chains (DOPC, POPC, OPPC and PCΔ6) but the same polar head were also studied. The results have shown differences in the both hydration and mobility of the membranes depending on the type of fatty acid chains of bilayer lipids. Finally, liposomes formed from cationic lipids, commonly used to deliver genes into cells in vitro and in vivo, were investigated. Measurements of the structure and dynamics of fully hydrated liquid crystalline lipid bilayers composed of the mixtures of cationic DOTAP and neutral DOPC with the use of fluorescence solvent relaxation technique were performed. The nonmonotonic dependence of dipolar relaxation kinetics (occurring exclusively on the nanosecond timescale) on DOTAP content in the membrane was found to exhibit a maximum integral mean solvent relaxation time at 30 mol % of DOTAP. Up to 30 mol %, the addition of DOTAP does not influence the amount of bound water at the level of the sn_1 carbonyls, but leads to an increased packing of phospholipid headgroup. Above this concentration, elevated lipid bilayer water penetration was observed. Additionally, to study the influence of hydrocarbon chain length and its saturation on membrane hydration and mobility, measurements similar as for DOTAP/DOPC were performed for the DMTAP/DMPC system.

CONTENTS

LIST OF PUBLICATIONS

The thesis is based on following publications (enclosed at the end of this thesis):

I. Piotr Jurkiewicz*, **Agnieszka Olżyńska***, Marek Langner and Martin Hof. Headgroup Hydration and Mobility of DOTAP/DOPC Bilayers: A Fluorescence Solvent Relaxation Study.
LANGMUIR (2006) 22, 8741-8749
* both authors contribute equally

II. **Agnieszka Olżyńska**, Anna Zań, Piotr Jurkiewicz, Jan Sýkora, Gerhard Gröbner, Marek Langner and Martin Hof. Molecular Interpretation of Fluorescence Solvent Relaxation of Patman and ^{2}H NMR Experiments in Phosphatidycholine Bilayers.
CHEMISTRY AND PHYSICS OF LIPIDS (2007) 147, 69-77

III. **Agnieszka Olżyńska**, Piotr Jurkiewicz and Martin Hof. Properties of Mixed Cationic Membranes studied by Fluorescence Solvent Relaxation.
JOURNAL OF FLUORESCENCE (2008) (published online)

IV. **Agnieszka Olżyńska**, Piotr Jurkiewicz and Martin Hof. Fluorescence Solvent Relaxation in Cationic Membranes.
In ANNUAL REVIEWS IN FLUORESCENCE 2008 (in press)

I confirm that results from publications and book chapter numbered I, II, III and IV (above) has not been used by me to get any other academic degree.

Other publications from the field of fluorescence:

V. **Olżyńska A**, Przybyło M, Gabrielska J, Trela Z, Przestalski S, Langner M, Di- and tri-phenyltin chlorides transfer across a model lipid bilayer, AOC 19 (2005) 1073-1078

VI. Jurkiewicz P, Sýkora J, **Olżyńska A**, Humpolíčková J, Hof M, Solvent relaxation in phospholipid bilayers: Principles and recent applications, J. FLUORESC. 15 (2005) 883-894

VII. Rieber K, Sýkora J, **Olżyńska A**, Jelinek R, Cevc G, Hof M, The use of solvent relaxation technique to investigate headgroup hydration and protein binding of simple and mixed phosphatidylcholine/surfactant bilayer membranes, BIOCHIM. BIOPHYS. ACTA – BIOMEMBRANES 1768 (2007) 1050–1058

VIII. Przybyło M, **Olżyńska A**, Han S, Ożyhar A, Langner M, A fluorescence method for determining transport of charged compounds across lipid bilayer, BIOPHYS. CHEM. 129 (2007) 120–125

IX. Jesenská A, Sýkora J, **Olżyńska A**, Brezovský J, Zdráhal Z, Damborský J, Hof M, Nanosecond Time-Dependent Stokes Shift at the Tunnel Mouth of Haloalkane Dehalogenases, submitted to JACS

X. Przybyło M, **Olżyńska A**, Hof M, Langner M, Direct affirmation of the lidocaine - membrane insertion model by solvent relaxation studies, submitted to BIOPHYS. CHEM.

ABBREVIATIONS

5-Doxyl	2-(3-carboxypropyl)-4,4-dimethyl-2-tridecyl-3-oxazolidinyloxy
16-Doxyl	2-(14-carboxytetradecyl)-2-ethyl-4,4-dimethyl-3-oxazolidinyloxy
DLS	dynamic light scattering
DMPC	1,2-dimyristoyl-sn-glycero-3-phosphocholine
DMTAP	1,2-dimyristoyl-3-trimethylammonium-propane
DNA	deoxyribonucleic acid
DOPC	1,2-dioleoyl-sn-glycero-3-phosphocholine
DOPE	1,2-dioleoyl-sn-glycero-3-phosphoethanolamine
DOTAP	1,2-dioleoyl-3-trimethylammonium-propane
FWHM	full width at half maximum
GUV	giant unilamellar vesicle
H_{II}	inverted hexagonal phase
HEPES	4-(2-hydroxyethyl)-1-piperazineethanesulfonic acid
IRF	instrument response function
L_{α}	liquid crystalline phase
Laurdan	6-dodecanoyl-2-dime-thylaminonaphthalene
LUV	large unilamellar vesicle
NMR	nuclear magnetic resonance
OPPC	1,2-oleoylpalmitoyl-sn-glycero-3-phosphocholine
Patman	6-hexadecanoyl-2-(((2-(trimethylammonium)ethyl)methyl)amino) naphthalene
PC	phosphatidylcholine
PCΔ6	1,2-dipetroselinoyl-sn-glycero-3-phosphocholine
POPC	1,2-palmitoyloleoyl-sn-glycero-3-phosphocholine
Prodan	6-propionyl-2-dimethylaminonaphthalene
SR	solvent relaxation (technique or process)
SUV	small unilamellar vesicle
Tempo-PC	1,2-dioleoyl-sn-glycero-3-phospho(Tempo)choline
TRES	time-resolved emission spectra

AIM OF THE STUDY

The history of fluorescence measurements of time-resolved emission spectra goes back 30 years. Up to date, the process of solvent relaxation monitored by fluorescence TRES was used to study solvation in neat solvents and their mixtures, hydration shells of proteins and also the dynamics of membranes. Since monitoring of the phospholipid bilayer hydration and mobility seems to be important for understanding their functions, SR method is undeniable a good choice. Although, a lot has already been done to improve the SR method and make the analysis more precise, researchers still face a number of difficult problems that must be analyzed with a great care in order to find the correct explanations for what they observe.

One of the examples, where SR technique can be very useful are cationic liposome measurements. Since the first described cationic liposome-DNA complex as non-viral transfection vector, the popularity of lipoplexes for both in vitro and in vivo applications seems to constantly increase. Unceasingly new molecules are being developed which are expected to improve transfection efficiency. Despite the impressive moving of the chemistry of the cationic lipid carriers, the process of delivery of lipoplexes is still very problematic. Many research groups working with the non-viral transfection vectors constantly face the fact that in some cases delivery based on cationic lipids works and in other cases it does not. As lipoplex design nowadays is mainly based on trials and errors, a lot of work on their structure and functions is still needed to better control transfection process. Therefore, getting more detailed knowledge on cationic liposome structure used in lipofection seems to be a good step. Positively charged compound, DOTAP, is a good candidate for above mentioned bilayer structural studies, since it is commercially available, not very expensive, the most widely used cationic lipid in both in vitro and in vivo applications.

Summarizing the above, the goals of this thesis were as follows:

- Determine the location of the number of fluorescent probes within model lipid membrane
- Choose the appropriate fluorescent dye for cationic liposome studies
- Understand better solvent relaxation on the molecular level
- Using solvent relaxation technique analyze the changes of cationic bilayer hydration and mobility caused by increasing positively charged molecule content
- Study the influence of the different lipid alkyl chains on the structure and dynamics of the cationic membrane

1. INTRODUCTION

1.1 BIOLOGICAL BILAYERS AND MODEL MEMBRANES

Lipid molecules together with many kinds of proteins and saccharides form membranes, the most fundamental structures in cells. Various membranes separate compartments inside the eukaryotic cells while plasma membrane provides the barrier that controls the communication between the cell and external world [1]. The composition of the biological bilayers varies from cell to cell, between two organelles within one particular cell and, additionally, lipids in the inner and outer leaflet of a membrane are usually distributed asymmetrically.

The most common components of biological membranes are phospholipids. These amphiphilic molecules with their hydrophobic (fatty acid tails) and hydrophilic (polar head) parts (Figure 1.1), create phospholipid bilayer (Figure 1.2) when put into the water.

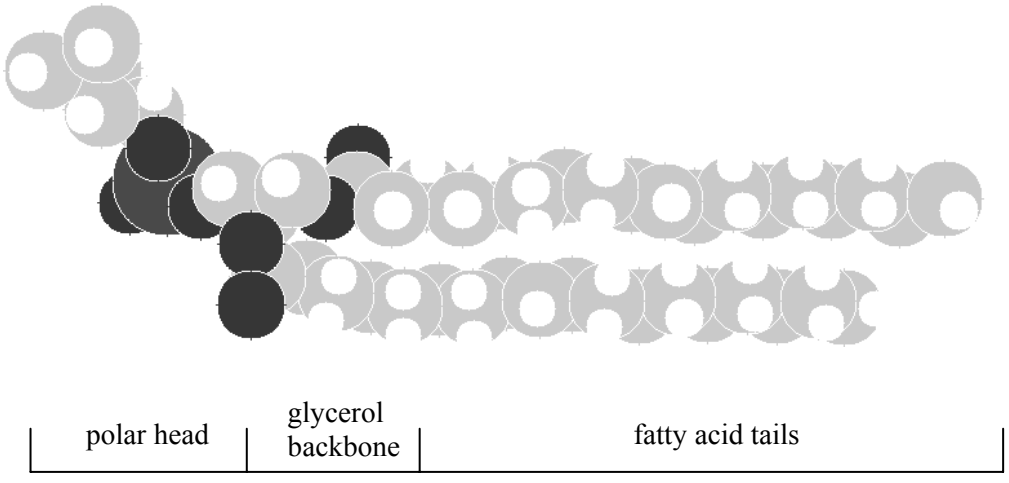

Figure 1.1 The atomic sphere model of phosphatidylcholine as an example of typical phospholipid.

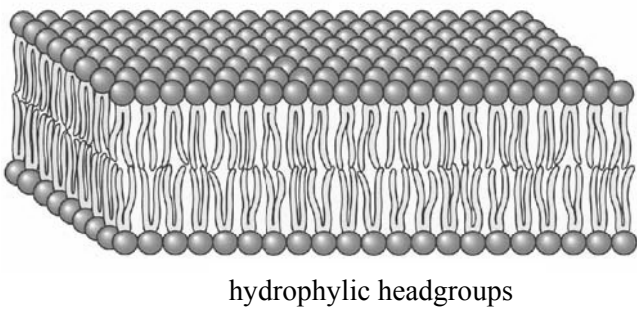

Figure 1.2 The structure of phospholipid bilayer alone.

The structure of phospholipid bilayer shown in Figure 1.2 is the simplified one. Real lipid membranes are dynamic systems governed mainly by weak interactions between molecules of water and amphiphilic lipids. Since biological membranes with all kinds of proteins and saccharides located in it are extremely complex and, as a consequence, quite difficult to study, model systems created from phospholipids seems to be the reasonable choice for experimental and theoretical studies. The motivation to investigate lipids and their aggregates comes from the fields of medicine, cell biology and physiology. Lipids, for instance, have been recognized as a convenient material for the targeted drug carriers [2-4], and recently, they become also the target of therapy [5], which confirms the need for extensive investigation of these compounds and structures they create.

1.1.1 Self-assembly of amphiphiles

The process of self-assembly of lipids into complex structures is mainly the result of the amphiphilic character of the molecules and the hydrophobic effect [1]. Since the water molecules tend to avoid contact with hydrocarbon chains of lipids, the different kind of lipid aggregates depending on the effective shape of the lipid molecules are created (Figure 1.3). Basically, lipid packing into aggregates with the polar group of the lipid molecule interacting with water via H-bonds and hydrophobic part buried inside the aggregate is determined by the volume and geometry of the molecule. Since amphiphiles forming membranes are not covalently bound, they can easily alter their arrangement upon a change of such physical parameters as temperature (thermotropic phase transitions) or the amount of solvent (lyotropic phase transitions) [6]. Because of the different proportions between the hydrophobic and hydrophilic part of the molecule

one can expect the particular amphiphilic aggregate shape when one knows the value of so-called packing parameter p described as [7]:

$$p = \frac{v}{al}, \tag{1.1}$$

where p is the volume of hydrocarbon part, a the area occupied by the headgroup, and l the maximum length of hydrocarbon chains. For example, when $p < 1/3$ (conical shape of the molecule), spherical micelles are created, while in order to obtain lipid bilayer it is necessary that $1/2 < p < 1$ (cylindrical molecular shape), and if $p > 1$ inverted hexagonal phase H_{II} forms (Figure 1.3) [8]. Among all the lipid aggregates, the lamellar phases are the most important from the biological point of view [9], however, non-lamellar phases have also been found in nature and are considered to be important for some biological processes.

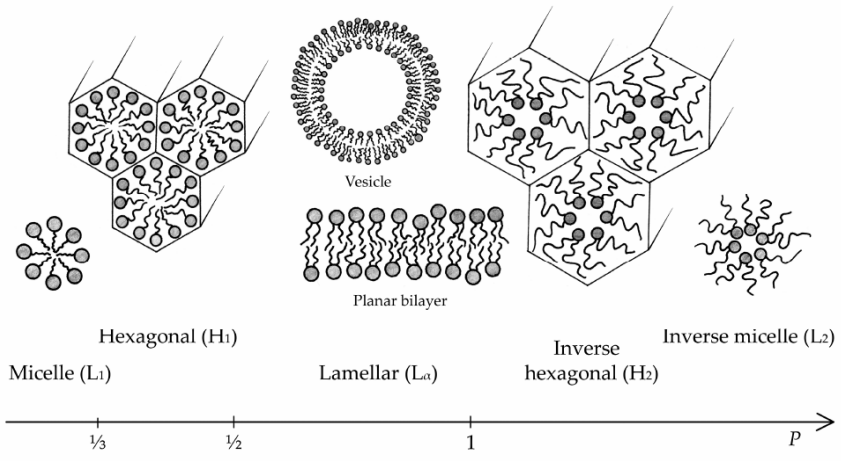

Figure 1.3 The common structures of the amphiphilic aggregates. The schemes of different phases are presented in the order of the packing parameter p, which characterizes the shape of the amphiphilic molecules (see Equation (1.1)).

1.1.2 Lipid vesicle - example of amhiphilic aggregate

Since the biological membranes are considered as too complex for both experimental and theoretical studies, model systems composed of the phospholipids are often introduced. The liposomes (spherical bilayers that enclose an aqueous compartment) are one of the examples. When water is added to phospholipids, multilamellar lipid vesicles (MLVs) heterogeneous both in size and shape form [10]. The sonication of MLVs produces small unilamellar vesicles, SUVs, with diameter

approximately 30 – 50 nm. Another way to obtain even more homogenous population of liposomes of bigger diameter is extrusion through polycarbonate filters with small pores [11]. Such large unilamellar vesicles, LUVs (Figure 1.4), can be prepared with diameter 50 – 1000 nm, depending on the pores size.

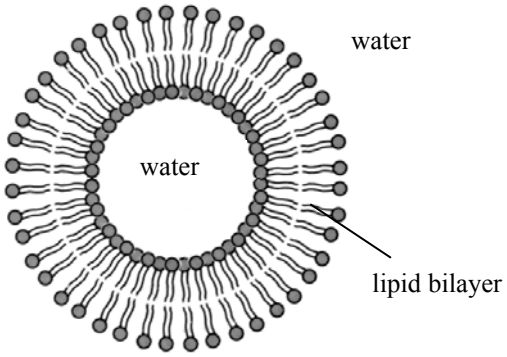

Figure 1.4 The cross section of the liposome bilayer.

Special kind of lipid aggregate represent giant unilamellar vesicles (GUVs), which diameters are in the range 5 - 200 μm. GUVs prepared by electroformation method, for instance, are frequently used to study lateral lipid organization [12, 13] .

1.1.3 Structure and hydration of lipid membranes

Lipid bilayer is a dynamic system and fluctuating constantly. Since the position occupied by lipid molecule instantly changes, it is rather impossible to determined one sharp border between the polar and non-polar part of lipid membrane.

To describe the structure of phospholipid bilayer the probability distribution function is often used [14, 15] (Figure 1.5, upper panel), however, more simplified, compartment representation also provides good description of the lipid membrane structure [16] (Figure 1.5, lower panel). In the case of the latter, the idea is based on dividing the bilayer into separate regions: “perturbed water”, “headgroup”, “soft polymer” and “decane”. The first region includes water molecules from the bulk that interact with the surface of the bilayer; the “headgroup region” is formed by the hydrated functional groups (carbonyls, glycerol, phosphate and cholines); the “soft polymer” region starts at the carbonyl groups and ends where the density of the chains

is comparable to liquid hexadecane; the "decane" region occupies the central part of a bilayer and is almost completely hydrophobic.

The properties of the hydrophobic interior of lipid bilayer are relatively easy to determine experimentally, but the lipid-water interface, where the polar headgroups of the lipids are located, is less explored [17, 18]. This is an unfortunate situation, since many biologically relevant processes, including interactions with nucleic acids, take place in this region. The headgroup region is characterized by large gradients of all relevant physicochemical parameters, providing a complex environment, which can be modified by both the alterations of lipid bilayer composition and properties of the aqueous phase [19]. This picture is further complicated by the dynamic character of the membrane, the components of which are free to undergo a variety of motions due to thermal agitation as well as macro-scale membrane movements that affect the bilayer and adjacent water layers [15, 20, 21]. Still relatively little is known about hydration and dynamics of lipid bilayer. The limited availability of experimental data suppress the development of lipid based technologies [22, 23].

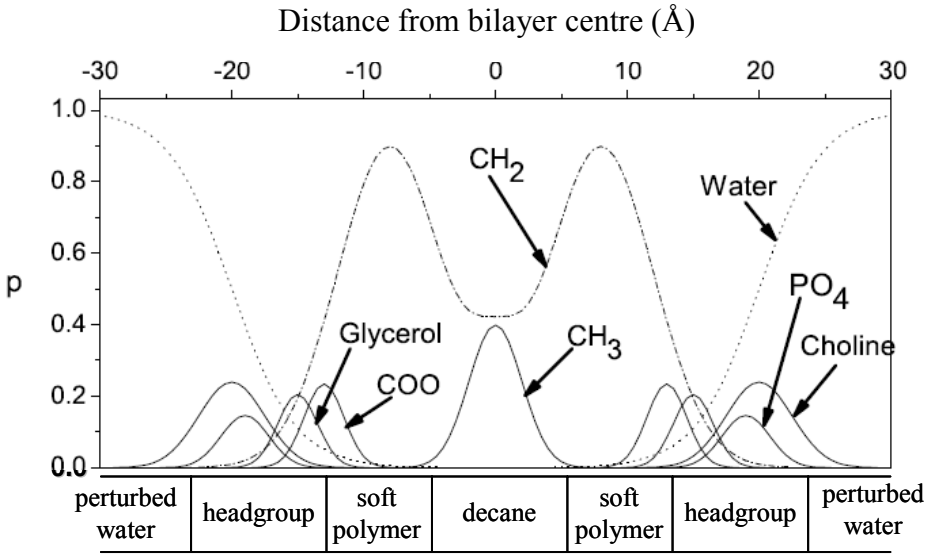

Figure 1.5 The distribution functions of the functional groups of a phospholipid along the z-axis of the bilayer obtained by theoretical simulations [14, 15] (upper panel) and the compartment representation of lipid bilayer (lower panel).

1.2 SOLVENT RELAXATION

Fluorescence methods, which are very popular in natural and model membrane studies, are capable of measuring numerous important parameters of lipid bilayer, such as local pH, concentrations of surface adsorbed compound, permeability, lateral and rotational diffusion of lipids, and others [17, 24-29]. Solvent relaxation technique (SR), based on simple time-resolved fluorescence measurements, when applied to lipid bilayers, is a unique tool that allows characterization of the bilayer hydration and mobility, the factors that are responsible for the state of the membrane and the way it interacts with its surroundings [30]. Among other techniques employed to study those parameters (e.g. NMR [31, 32], fluorescence [33, 34], X-ray, and neutron diffraction [35, 36]) the solvent relaxation is unique in its ability to measure fully-hydrated free-standing liquid crystalline lipid bilayers, which are the most biologically relevant membrane models [37-39].

1.2.1 Phenomenon of solvent relaxation

As it has been already mentioned, solvent relaxation technique enables to characterize the hydration and mobility of fully-hydrated free-standing lipid bilayers [30, 37, 39, 40]. This can be achieved by monitoring the so-called time resolved emission spectra (TRES).

When fluorophore absorbs photon, its electrons are redistributed in a very short time which results in a change in the dipole moment. At the same time, the displacement and reorientation of the position of the surrounding solvent molecules does not occur. Therefore, after excitation the dipoles of solvent molecules, which have been in the equilibrium with the dye in the ground state, are forced to adapt to the new situation and reorganize in order to reach a relaxed state of minimum free energy (Figure 1.6). As a consequence of the presence of the "solute–solvent" interactions, the energy of the state from which the dye emits is different from that of the Franck-Condon one. The dynamic process starting from the initial non-equilibrium Franck-Condon state and gradually proceeding toward the fully relaxed state is called solvent relaxation. The higher the polarity of the solvent, the lower the energy of the relaxed state and the larger the red-shift of the emission spectrum. This continuous red-shift caused by the relaxation

process can be monitored by recording, already mentioned, time resolved emission spectra (TRES).

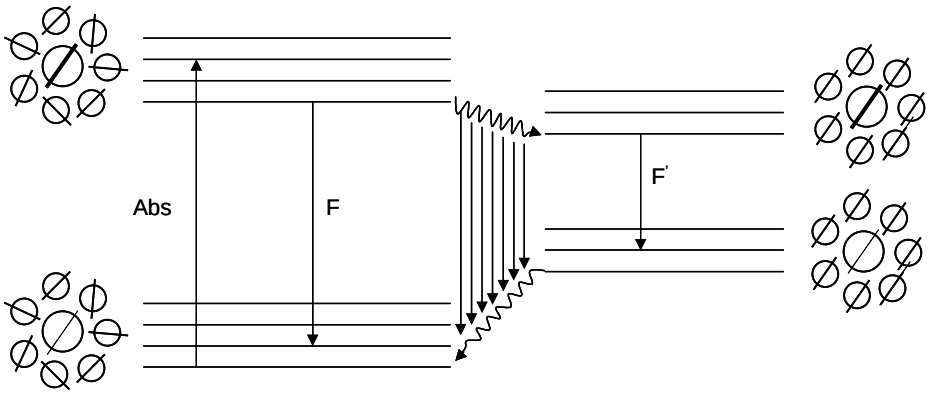

Figure 1.6 Schematic diagrams presenting solvent relaxation around a probe that has a weak dipole moment in the ground state and a large dipole moment when excited. The reorientation motion of the solvent molecules leads to the lowering of the energy of the system resulting in the red shift of monitored TRES.

1.2.2 Information gained from TRES

The analysis of the time-resolved emission spectra (TRES) enables to extract the solvent relaxation information from the fluorescence signal. TRES are obtained by the spectral reconstruction method [41] and fitted by a log-normal function in order to determine the position of the spectra $\nu(t)$ (in terms of their maxima) and their full widths at half maxima (FWHM).

The two main factors that can be extracted from TRES are the total spectral shift (i.e. how far the emission spectrum is shifted during the whole process) and its kinetics (i.e. how fast the spectrum is shifting).

The overall shift $\Delta\nu$ is attributed to the difference between the energies of the Frank-Condon and the fully relaxed state, which are proportional to $\nu(0)$ (t=0) and $\nu(\infty)$ (t=∞), respectively [41] and defined as:

$$\Delta\nu = \nu(0) - \nu(\infty), \tag{1.2}$$

The second information can be obtained calculating the spectral response function (or correlation function), defined as:

$$C(t) = \frac{\nu(t) - \nu(\infty)}{\nu(0) - \nu(\infty)} = \frac{\nu(t) - \nu(\infty)}{\Delta\nu}, \tag{1.3}$$

by taking the estimated time-zero spectrum as $\nu(0)$. The so-called time-zero spectrum is the hypothetical fluorescence emission spectrum of the dye which is vibrationally

relaxed but emit before any nuclear solvent motions occur. As has been shown, this spectrum cannot be measured directly in most systems due to the finite temporal resolution of the apparatus, but can be estimated using absorption and steady-state emission spectra measured in a non-polar solvent [40]. A comparison of the positions of time-zero spectra (the estimated and reconstructed one) also allows the percentage of the solvation process below the time resolution of the experimental setup to be determined [42, 43]. In order to quantitatively characterize the solvent relaxation process, two parameters defined above are analyzed. It has been shown that $\Delta\nu$ is proportional to the polarity of the dye environment [41]. In a phospholipid/water system, polarity is mainly attributed to water molecules, therefore $\Delta\nu$ reflects the extent of lipid bilayer hydration. For Prodan, Laurdan, and Patman, which share the same fluorophore and time-zero spectra, the uncertainty of 50 cm^{-1} for comparing the $\Delta\nu$ values is assumed.

The second parameter assigned to a relaxation process is the relaxation time, which describes the mobility of the solvent molecules, and is interpreted as a measure of the viscosity for neat solvents [41]. In the phospholipid bilayer at the level of glycerol, however, water hydrating the membrane is fully bound to the phospholipid molecules. Therefore, the slow relaxation kinetics observed in membranes is attributed to the collective relaxation of the dye environment and reflects membrane dynamics rather than the motions of water molecules [42, 43]. The integrated mean solvent relaxation time can be calculated according to the following formula:

$$\tau_r \equiv \int_0^\infty C(t)dt \tag{1.4}$$

Above approach does not require any *a priori* knowledge about the solvation process [41] unlike fitting the relaxation function by kinetic models [42, 44]. The intrinsic uncertainty of this parameter was assumed to be ~ 20 ps, based on the time resolution of the experimental setup.

The temporal behavior of the FWHM of the TRES provides useful information on the extent of the observed solvent relaxation. The experiments carried out in phospholipid bilayers [45, 46] and also in the supercooled liquids [47] have shown that the FWHM passes a maximum during solvation process. This is in a good agreement with the idea of a non-uniform spatial distribution of solvent response times [47, 48]. It has been shown that in homogeneous systems of low molar mass molecules, the FWHM

decays monotonically. In a spatially inhomogeneous systems, however (i.e. where the microenviroments of the fluorophores differ), the relaxation behavior is different, since the solvent shells of individual fluorophores distributed in the system, respond with different rates to changes in the local electric field (which also spatially varies). This gives rise to a new phenomenon, which reflects the time distribution of phases of relaxations of individual solvation shells during the relaxation. The overall transient inhomogeneity increases significantly during the solvation and than decreases once the solvation finishes and the equilibrated excited state is reached. That is why the FWHM of TRES, which gives the measure of inhomogeneity of dyes microenvironments, passes a pronounced maximum. This effect gives the origin for the method of checking whether the entire response or merely part of it was captured within the time-window of the experiment. If only a decrease in the FWHM is observed, it means that the early part of the relaxation process is possibly beyond the time resolution of the equipment. In contrast, if only an increase is detected, the process is fairly slow under given conditions and the lifetime of the used fluorophore is not long enough to completely monitor the relaxation. It should be mentioned that in the case of Aerosol-OT reverse micelles, it is suggested from experiment [49] and by computer simulations [50] that the time dependence of the FWHM is due to self-diffusion of the excited probe (4-(dicyanomethylene(-2-methyl-6(*p*-dimethylaminostyryl)-4*H*-pyran) from non-polar to polar location. However, since the chromophores of Laurdan and Patman are anchored in the hydrophobic part of the bilayer, this alternative explanation appears unlikely for the lipid experiments presented here.

1.2.3 SR probes - naphthalene derivatives

It has been already mentioned that the solvent relaxation dyes should undergo a large change in their dipole moment upon excitation (large Stokes shift). In the lipid membranes there are, however, further requirements that should be imposed on fluorescent probes. First of all, the chromophore has to be incorporated into the lipid bilayer, which usually requires that the probe be at least partly hydrophobic. It is very important to know the exact location and position of the chromophore in the bilayer, and to assure that these are not changed during experiment. Finally, the size and the structure of the probe should disturb the bilayer as little as possible; from the same reason the quantum efficiency should be high enough to keep the dye to lipid ratio low.

Solvent relaxation in the lipid membranes is four decades slower than in the bulk water – the mean time constant in pure water is about 0.3 ps [51], whereas at the glycerol level of a fully hydrated phospholipid bilayer in the liquid crystalline state it is about 2 ns [42]. Such a large change in solvation kinetics on a distance of only 1 nm results in enormous gradients of solvation properties along the membrane normal. Knowledge about the precise location of a polarity-sensitive fluorescent dye is crucial for characterization of the relaxation properties. It is also very advantageous if one has a series of probes with the same chromophore located at different depths within the bilayer. Examples of such dyes include naphthalene derivatives Prodan, Laurdan and Patman (Figure 2.2), which are often used in our laboratory. Their fluorophore consist of the electron-donating dimethylamino group and the electron-withdrawing carbonyl group of a different fatty acid residue, separated by a naphthalene ring. The naphthalene ring ensures a substantial increase of dipole moment upon electronic excitation.

Prodan [52], which contains a short propionyl group, is believed to be located in the outermost region of the interface [53]. The location is, however, poorly defined and, consequently, any measurements performed with Prodan should be always evaluated with care (see [54], for example). In addition, there was hypothesized that the two population of this probe that differ in their positions can be present in membrane: one perpendicular and one parallel to the membrane surface [53]. It is also the most water soluble dye from the set, hence some of the fluorescence signal can originate from the bulk which further complicates the interpretation of results. Nevertheless, Prodan is still a valuable membrane probe and can be successfully used in solvent relaxation studies [37, 54, 55].

Laurdan and Patman molecules are modified so that their location within the membrane is more stable. Laurdan has a longer hydrocarbon chain (11 carbons) attached to the carbonyl group, which anchors the molecule in the hydrophobic part of the bilayer. It is commonly assumed that its fluorophore stays at the level of the glycerol backbone [56]. This assumption is a result of a comparison between its fluorescence properties under different experimental conditions [56-58].

Patman, in addition to a palmitoyl tail, possesses a trimethylammonium group, which orients the alkylamino end of the fluorophore toward the lipid-water interface [59] and stabilizes the dye position in the bilayer due to interactions with charged phospholipid headgroups. The location of Patman is stable and unimodal. The NMR

studies have shown that Patman is embedded deeper in the bilayer compared to Prodan, and that its movement is more restricted [38]. The positive charge of the ammonium group can be a serious drawback of this probe in some applications.

1.3 NON-VIRAL GENE TRANSFER VECTORS

1.3.1 Cationic liposomes in transfection

The interest in positively charged lipid membranes stems from biology, where cationic lipids are used for delivery of nucleic acids into host cells to achieve transgene expression or gene regulation – techniques that are essential for genomics and proteomics. Electrostatic interaction of polyanionic DNA or RNA with cationic lipids leads to formation of the so-called lipoplex, which functions as a transfection vector [60-63]. Complexation with lipids facilitates the cell uptake of genetic material, in particular crossing the hydrophobic barrier of cellular membrane. The efficiency of lipofection is still lower than transfection with viral vectors, but this is the safety and biocompatibility that drew attention to the lipofection in medicine. The long-term potential of gene therapy for the treatment of both inherited and acquired disorders is the motivation for many studies on transfection agents. The focus in lipid vector development is on protecting genetic material from degradation in the bloodstream of a patient (e.g. stealth liposomes), selectively targeting vector to the cells of interest, increasing transfection efficiency, and maintaining stability and repeatability of the formulation. All these require a thorough knowledge about the lipoplex structure and its interactions with physiological environment. Although, it is already more than 20 years since cationic lipids were first used in DNA delivery in tissue cultures [64], still little is known about the possible structures of the lipoplexes and how the structure is determined by the lipid composition and physicochemical parameters. There are likely other factors besides electrostatics [65] that should be considered to better control the association process. The lipids that are used to form a lipoplex are usually mixtures of at least two lipid species in a form of liposomes (unilamellar or multilamellar). Moreover, the lipid surface is commonly altered by modifying the positively charged lipid compound [60, 66, 67] or grafting the surface with a polymer [68-70]. No quantitative measure of such alterations exists, therefore, the approach is usually reduced to trial and error. It is reasonable to study the structure and properties of the mixed cationic lipid membrane itself before characterizing their interactions with nucleic acids and the structure and function of the resulting lipoplex. Basic studies on positively charged lipid membranes are relatively new, since the main interest was, for a long time, on neutral

and negatively charged lipid bilayers, which are omnipresent in natural membranes, in contrast to the positive ones, which are rare in nature.

1.3.2 DOTAP surfactant

Cationic lipids used in transfection protocols are synthetic products like, synthesized in 1988, DOTAP [71]. This monocationic quaternary surfactant consists of amine-based cationic headgroup which is connected to two unsaturated hydrocarbon chains through the linker (Figure 1.7.). This positively charged lipid alone or when mixed with DOPC tends to form bilayer (liposomes) and since DOTAP phase transition temperature is -11.9°C [72], the liposomes are easily formed at room temperature. The superiority of DOTAP over its analogues stem from the experiments showing better transfection activity when considering different kinds of amines present in monocationic surfactants [73]. Moreover, lipid formulation containing compound with the ester bond, like in DOTAP, was found to be less toxic than with ether or carbamate one [74, 75]. The pH-independence of the positive charge of the DOTAP molecule [76] is also of great importance since cationic charge is critical for efficient DNA binding, cellular lipoplex uptake, and trafficking. Another advantage of the DOTAP formulations is its good stability [77] that is preserved for more than 3 years when DOTAP liposomes are stored as dry lyophilized powder at 4 °C.

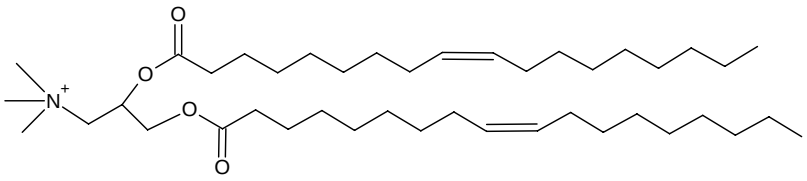

Figure 1.7 Structure of the DOTAP molecule.

2 MATERIALS AND METHODS

2.1 MATERIALS

Zwitterionic phospholipids: 1,2-dioleoyl-*sn*-glycero-3-phosphocholine (DOPC), 1,2-dipetroselinoyl-sn-glycero-3-phosphocholine (PCΔ6), 1,2-oleoyl-palmitoyl-*sn*-glycero-3-phosphocholine (OPPC), 1,2-palmitoyloleoyl-*sn*-glycero-3-phosphocholine (POPC), 1,2-dimyristoyl-*sn*-glycero-3-phosphocholine (DMPC) and cationic: 1,2-dioleoyl-3-trimethylammonium-propane chloride (DOTAP) and 1,2-dimyristoyl-3-trimethylammonium-propane (DMTAP) used in this study were supplied by Avanti Polar Lipids, Inc. (Alabaster, AL, USA) (Figure 2.1). All lipids were stored in chloroform at -20°C and used without further purifications.

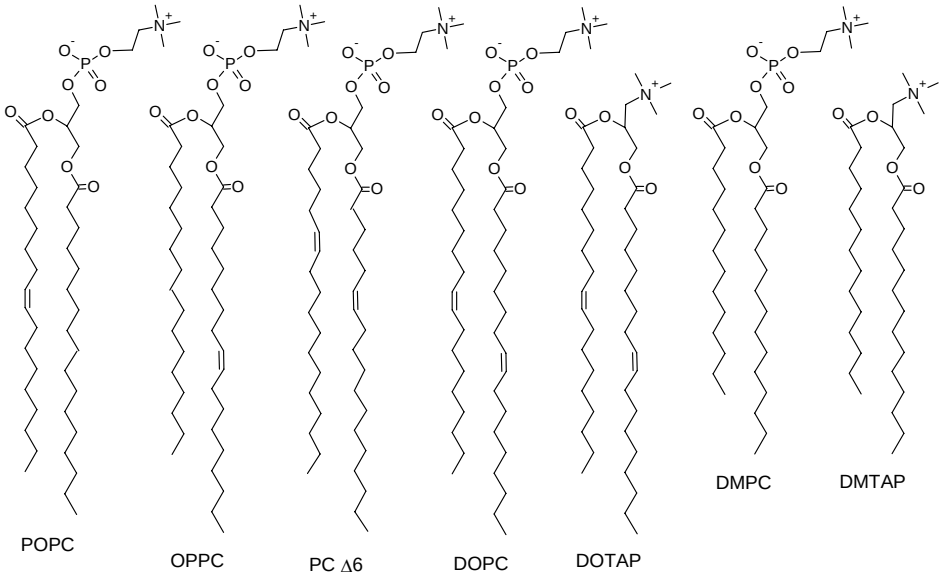

Figure 2.1 Structures of the lipids used in this study.

Napthalene derivatives: 6-hexadecanoyl-2-(((2-(trimethylammonium)ethyl)methyl) amino)naphthalene chloride (Patman), 6-dodecanoyl-2-dimethylaminonaphthalene (Laurdan) and 6-propionyl-2-dimethylaminonaphthalene (Prodan) used in this study were purchased from Molecular Probes (Eugene, OR, USA) (Figure 2.2).

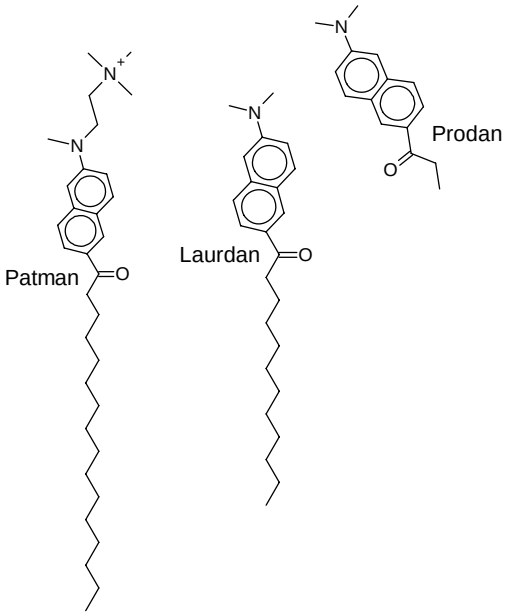

Figure 2.2 Structures of the fluorescent probes used in this study.

The spin-labeled quencher molecules 1,2-dioleoyl-*sn*-glycero-3-phospho(TEMPO)choline (TEMPO) was obtained from Avanti Polar Lipids, Inc. (Alabaster, AL, USA); 2-(3-carboxypropyl)-4,4-dimethyl-2-tridecyl-3-oxazolidinyloxy (5-Doxyl-stearic acid) and 2-(14-carboxytetradecyl)-2-ethyl-4,4-dimethyl-3-oxazolidinyloxy (16-Doxyl-stearic acid) were supplied from Aldrich (Steinheim, Germany). Acrylamide was ordered from Fluka (Buchs, Switzerland).

Hepes was purchased from Fluka (Buchs, Switzerland). Solvents of spectroscopic grade were supplied from Merck (Darmstadt, Germany).

2.2 METHODS

2.2.1 Vesicle preparation

Lipid vesicles were prepared in a glass tube by mixing required volumes of the chloroform solution of the lipid with the methanol solution of selected fluorescent dye. The final concentration of the probe in all samples was 1 mol %. Solvents were evaporated under a stream of nitrogen while being continuously heated. To remove residual solvent, samples were kept under high vacuum over night. The dry lipid film was hydrated with 10 mM HEPES buffer (pH=7.4, 100 mM NaCl) and vortexed for 4 minutes. Large Unilamellar Vesicles (LUVs) were formed by extrusion through a polycarbonate membranes (Avestin, Ottawa, Canada) with 100 nm pores [11]. Prepared samples were transferred to a 1 cm quartz cuvette and equilibrated at the desired temperature for 10 minutes before measurement. Unless otherwise specified, the final concentration of the lipid in the sample was 1 mM.

In the case of cationic liposomes, where positively charged lipid (DOTAP or DMTAP) content in the bilayer was from 0 to 100 mol %, total lipid concentration was kept constant. Multilamellar Vesicles (MLVs) for the parallax measurements was containing in their membrame 15 mol% of selected spin-labeled compound.

2.2.2 Steady-state fluorescence measurements

All steady-state excitation and emission spectra acquisition were performed on a Fluorolog-3 spectrofluorometer (model FL3-11; Jobin Yvon Inc., Edison, NJ, USA) equipped with a Xenon-arc lamp. The spectra were collected in 1 nm steps (2 nm bandwidths were chosen for both the excitation and emission monochromators). The temperature in the cuvette holder was maintained within ±0.1°C using a water-circulating bath.

2.2.3 Fluorescence quenching with acrylamide

Fluorescence quenching measurements were performed with a Fluorolog-3 spectrofluorometer. The LUVs suspension (0.08 mM lipid concentration) was transferred to a quartz cuvette and thermostated at 20 ^{o}C for at least 10 min, while being

constantly stirred. Fluorescence intensity changes were measured after sequentially additions of the small amounts of 5 M stock solution of acrylamide in water to liposome suspension. The excitation wavelength used was 373 nm and emission was monitored at the maximum of the emission spectrum. Quenching data were analyzed using the Stern-Volmer equation [78]:

$$\frac{F_0}{F} = 1 + K_D[Q], \tag{2.1}$$

where F_0 and F are the fluorescence intensities in the absence and presence of the quencher, respectively, K_D is the Stern-Volmer quenching constant, and [Q] is the concentration of the quencher in the sample.

2.2.4 Parallax fluorescence quenching

The parallax analysis of fluorescence quenching was used to determine the positions of the fluorescent probes within the membrane [79, 80]. Steady-state fluorescence measurements were carried out on a Fluorolog-3 spectrofluorometer. In brief, 1 mol% of the dye was added to the lipid mixture with or without 15 mol % of one of the three free radical quenchers (TEMPO, 5-Doxyl-stearic acid, 16-Doxyl-stearic acid) present. The steady-state fluorescence intensity as well as fluorescence decays were measured at different emission wavelengths. Data collected for the three quenchers was analyzed in pairs, in order to obtain the distance h of the dye from the bilayer centre, according to [80]:

$$h = \frac{\pi C\left(h_{q1}^2 - h_{q2}^2\right) - \ln\left(\frac{F_1}{F_2}\right)}{2\pi C\left(h_{q1} - h_{q2}\right)}, \tag{2.2}$$

where F is the fluorescence intensity in the presence of quencher, and h_q is the distance of the quencher from the bilayer center. The subscripts designate different quenchers, and C indicates the surface concentration of the quencher in molecules per unit area. The results obtained for different pairs of quenchers were collected and compared.

An alternative method is to calculate the distribution function of the quenched dye by fitting the collected data for three quenchers with the parallax profile:

$$\ln\left(\frac{F_0}{F(h_q)}\right) = \begin{cases} \pi C\left[R_c^2 - \left(h_q - h\right)^2\right] & : \; h_q - h < R_c \\ 0 & : \; h_q - h \geq R_c \end{cases}, \tag{2.3}$$

where F_0 is the fluorescence intensity in the absence and $F(h_q)$ in the presence of the quencher located at a distance h_q from the bilayer center, and R_c is the radius of quenching [81].

2.2.5 Time-resolved fluorescence measurements

Fluorescence decays were recorded on a 5000U Single Photon Counting setup (IBH, Glasgow, UK), using an IBH laser diode NanoLED 11 (370 nm peak wavelength, 80 ps pulse width, 1 MHz maximum repetition rate) and a cooled Hamamatsu R3809U-50 microchannel plate photomultiplier. Emission decays were recorded at a series of wavelengths spanning the steady-state emission spectrum (usually 400 nm – 540 nm) in 10 nm steps (emission slits: 8 nm bandwidths). Additionally, a 399 nm cutoff filter was used to eliminate scattered light. The signal was kept below 2 % of the light source repetition rate (1 MHz). Data was collected in 8192 channels (0.014 ns per channel) till the peak value reached 5000 counts. The time resolution, calculated as 1/5 of the full width at half maximum (FWHM) of the instrument's response function (IRF), was about 20 ps. Fluorescence decays were fitted to multi-exponential functions (2 or 3 exponential components were used), using the iterative reconvolution procedure with IBH DAS6 software.

2.2.6 Dynamic light scattering

The size distribution of vesicles was measured using Dynamic Light Scattering (DLS). The light scattering setup (ALV, Langen, Germany) consisted of a 633 nm He-Ne laser, an ALV CGS/8F goniometer, an ALV High QE APD detector, and ALV 5000/EPP multibit, multitau autocorrelator. Prior to measurement, samples were filtered through 0.45 μm Acrodisc filters. Experimental, normalized intensity autocorrelation functions were analyzed using cumulant analysis [82] and constrained regularized fitting based on the CONTIN method [83]. Mean vesicles sizes, along with the standard deviation, were calculated from surface weighted size distributions.

3 RESULTS AND DISCUSSION

3.1 SR PROBES LOCATION IN LIPID BILAYERS

Easy and efficient tools to experimentally determine chromophore location within the lipid membrane are fluorescence quenching techniques. One of them is the parallax method, which can be used to measure the mean distance of the fluorophore from the bilayer centre [27, 79, 80]. For the polarity sensitive probes located within the membrane interface a better measure of their distribution can be obtained with wavelength-dependent parallax quenching.

The paralax method was used to measure Laurdan and Patman locations in DOPC bilayer. The distance from the bilayer center and the mean location of Laurdan fluorophore, calculated using equation 2.2, was about 11.4 Å, regardless of the selected pair of quenchers. The obtained value was comparable to 9.8 Å measured in the cell membrane of Torpedo marmorata enriched with nicotine acetylcholine receptors [84]. The radius of the sphere of quenching, calculated according to equation 2.3, was equal to 12.8 Å, again in good agreement with values reported elsewhere [80]. The distance measured for Patman was 10.4 Å from the bilayer centre. The results obtained for Prodan for different pairs of quenchers were not consistent and suggested a broad distribution of this dye. The statistical character of the location of both Laurdan and Patman and also quenchers implies that all the obtained values are averages and that the actual values can fluctuate [79]. The determined position of the two dyes are indicated in the schematic lipid bilayer representation in Figure 3.1, together with the hypothetical Prodan position found in the literature [56].

The difference in location between the chromophores of Patman and Laurdan is 1 Å, which is close to the uncertainty of the parallax method, but agrees with the SR results obtained for these probes in many lipid systems. It must be kept in mind that this small 1 Å difference in position occurs in the bilayer region where a large gradient of water

concentration is present [15]. This fact, together with the sensitivity of the solvent relaxation method, is responsible for the differences in the measured relaxation times and $\Delta\nu$ values.

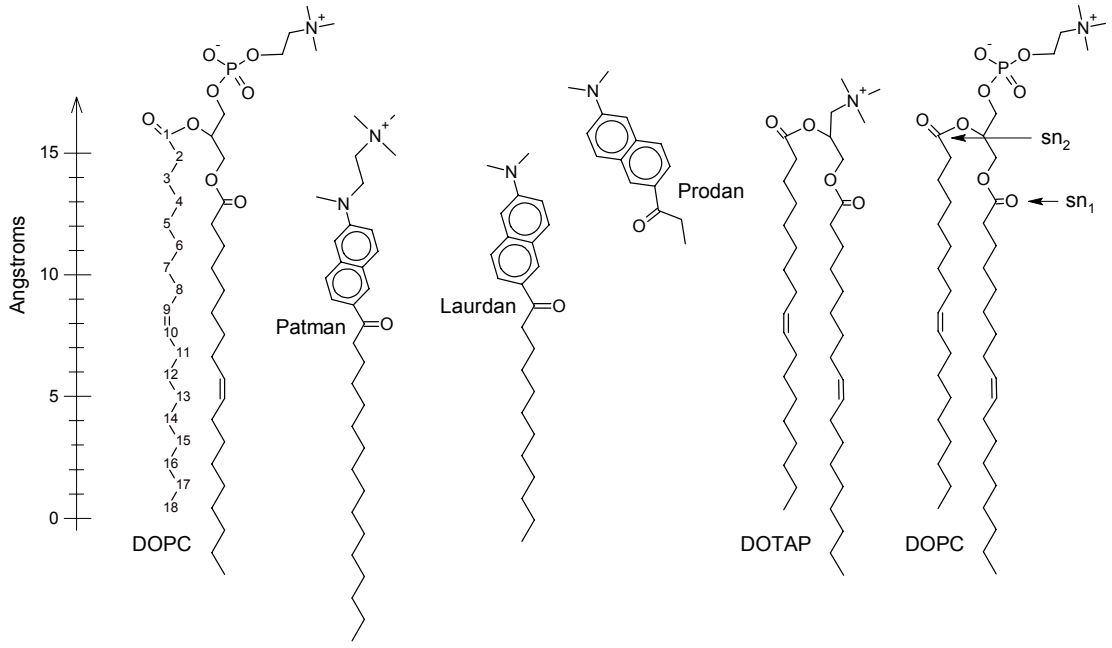

Figure 3.1 Schematic diagram of the location of Patman, Laurdan and Prodan in a membrane composed of DOPC and DOTAP. The positions of sn_1 and sn_2 carbonyls are indicated by arrows. The carbon atoms of the sn_2 chain are numbered. The scale on the left shows the approximate distance from the bilayer center. Upon the addition of DOTAP, the position of Patman changes and differs from the one shown here. See the text for details on the dye locations.

The average positions of Laurdan and Patman were determined for the emission maxima, i.e. 493 nm and 475 nm, respectively. A strong dependence of quenching efficiency on the emission wavelength was observed. The calculated distances of the dyes from the membrane centre increased with the wavelength (Figure 3.2).

An increase in the detection wavelength of the emission leads to the photoselection of the chromophores, which are in a more relaxed and/or more polar environment, since solvent relaxation becomes faster and the amount of water increases when moving towards the lipid/water interface [39]. Thus, the wavelength dependence of the quenching rate provides information on the heterogeneity of the chromophore locations along the bilayer normal. These two dyes differs in this respect, i.e. a stronger dependence of the calculated position on the emission wavelength is observed for Laurdan (~2 Å) than for Patman (<1 Å). This can be a result of the presence of the trimethylammonium group and longer hydrophobic chain in the molecule of Patman.

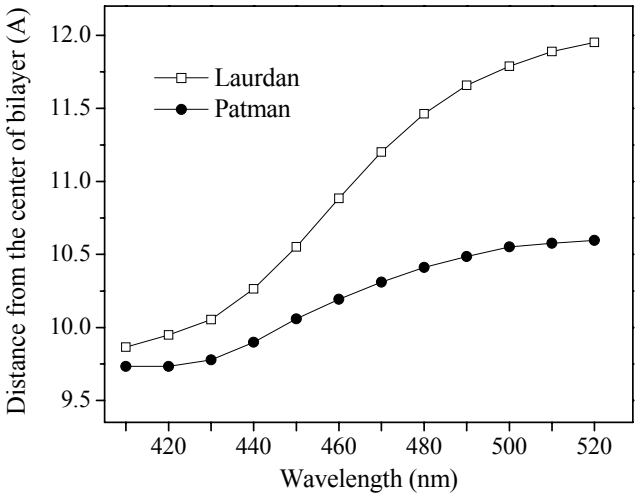

Figure 3.2 Position of Laurdan (open squares) and Patman (filled circles) in terms of the distance from the centre of bilayer, calculated according to equation 2.2 for different emission wavelengths. The dye was excited at 373 nm. The measurements were performed at 20 °C.

Once the location of a probe within lipid bilayer of interest is known, one can check if it is stable upon the changes in composition or physicochemical parameters. The easiest way to do this is to quench the fluorescence using a quencher that is water soluble and does not penetrate lipid membrane. One of such quenchers is acrylamide. Because of its neutral charge, it was selected to check whether the addition of cationic lipid DOTAP to the DOPC lipid bilayer does not change the locations of the probes. The fluorescence intensity was being measured while the sample was titrated with the quencher. The data were analyzed in terms of the Stern-Volmer equation (Equation 2.1). Only the quenching plots for Prodan departed slightly from linearity, which is yet another indication for a rather heterogeneous localization of this probe [53, 85]. The Stern-Volmer constants obtained for Laurdan and Patman are summarized in Table 3.1. An interesting result was the relocation of Patman, which moved out of the bilayer when the content of DOTAP was changed from 0 to 30 mol%. Further addition of DOTAP did not change the position of Patman any further. In the case of Laurdan there is no significant change in its position. The increased accessibility of the fluorophore to acrylamide might also be explained by the increased penetration of the quencher into the interfacial region of the lipid bilayer. In such case, however, we would have observed the same effects for both dyes. Additionally the scenario of increased membrane penetration is unlikely in the view of the SR results, which indicate that the

membrane becomes tighter when the amount of DOTAP rises to 30 mol%. In conclusion, the observed rise in the quenching efficiency for Patman is a consequence of its relocation upon the addition of DOTAP (up to 30 mol%).

Table 3.1 The quenching of Patman and Laurdan embedded in DOPC/DOTAP LUVs with acrylamide.

[DOTAP] (mol %)	Patman	Laurdan
	K_D (M^{-1}) [(a)]	K_D (M^{-1}) [(a)]
0	0.274 ± 0.003	0.340 ± 0.005
30	0.314 ± 0.003	0.347 ± 0.004
50	0.317 ± 0.004	0.350 ± 0.006
100	0.314 ± 0.006	0.369 ± 0.003

[(a)] K_D – Stern-Volmer constants calculated by fitting the data points to a straight line.

In addition to the quenching techniques, the analysis of the TRES width can give an indication whether the distribution of the probe fluorophore within the membrane is unimodal. We showed that if more than one homogenous population of the dye is present, or if other processes, besides solvation, take place, the FWHM profile clearly differs from the one normally observed [39, 42, 54].

3.2 Influence of the lipid hydrocarbon chain structure on the membrane dynamics

Solvent relaxation measurements were performed for four lipid systems (DOPC, POPC, OPPC and PCΔ6) (see Figure 2.1) in order to investigate the influence of the structure of the acyl chains of lipids on the membrane dynamics. Patman, located slightly below the level of the hydrated ester-group of the sn_1 lipid chain (see Section 3.1), was chosen as a suitable dye for the studies since acrylamide experiments showed that its location was not changed by the chemical nature of the chains of electrically neutral lipids.

It was shown that the solvation dynamics in lipid bilayers becomes faster with increasing temperature [26]. This trend is visible when comparing the SR characteristics in a particular bilayers system at different temperatures. Trivially increasing temperature leads to higher headgroup mobility. On the other hand, in four investigated lipid systems (i.e. DOPC, POPC, OPPC and PCΔ6 bilayers), the $\Delta\nu$ values are invariant with the temperature, indicating that the level of hydration in the vicinity of the chromophore does not change within the examined temperature range. When comparing lipids with different phase transition temperatures, T_m, the measurements are often performed at certain temperature offset above that phase transitions of these lipids (at the so-called relative temperatures). It is also assumed that at the certain temperature (above T_m of both compared lipids) the dynamics of the lipid with lower T_m should be faster. This assumption holds true, when comparing DOPC with either POPC or OPPC measured at, for instance, 10 ^{o}C and 25 ^{o}C. Considering the T_m values of those lipids [86] it is understandable that the SR curve for DOPC (T_m = -18.3 ± 3.6 ^{o}C) decreases considerably faster than for POPC (T_m = -2.5 ± 2.4 ^{o}C) and OPPC (T_m = -8.9 ± 0.7 ^{o}C) (Figure 3.3). Hovewer, when the OPPC and POPC isomers are compared, the faster relaxation is observed for POPC, for which the difference between phase transition temperature and the temperature at which measurements are performed is smaller (Figure 3.3).

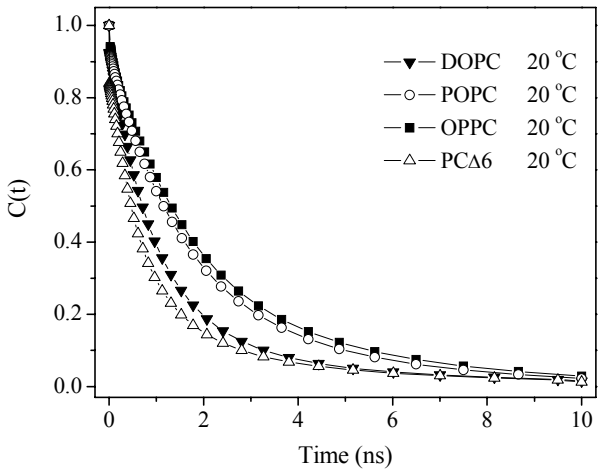

Figure 3.3 Correlation functions for Patman in DOPC (▼), POPC (○), OPPC (■), PCΔ6 (△) LUVs. Measurements were performed at 20 °C.

The difference in the solvent relaxation kinetics between OPPC and POPC becomes even more evident when measured at the temperatures relative to the phase transition (Figure 3.4). In this case (OPPC measured at 20 °C K and POPC measured at 27 °C; in other words ~ 30 °C above their phase transitions), the difference in the relaxation times between the two lipids reaches 30%. We attribute these results to the different depth of double bond position in the POPC and OPPC bilayers. The double bond containing chain in POPC is attached at the sn_2 position, which is located closer to the water phase (see Figure 2.1) than the sn_1 (which is the attaching point for the OPPC double bond containing chain). Thus, in POPC the double bond is located closer to the glycerol level, where the Patman resides, which explains why the faster SR kinetics is observed.

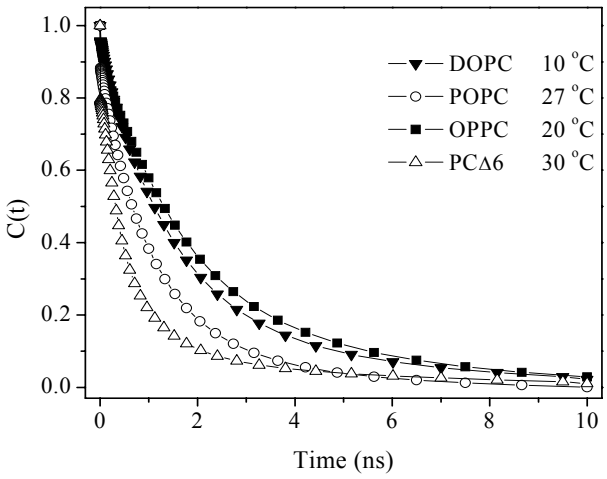

Figure 3.4 Correlation functions for Patman in DOPC (▼), POPC (○), OPPC (■), PCΔ6 (△) LUVs. Measurements were performed at temperatures relative to the transition temperatures T_m of the lipids.

In order to investigate the influence of the position of the double bonds within the acyl chains on the solvent relaxation kinetics of Patman, measurements in PCΔ6 liposomes were performed. While DOPC contains double bonds at 9th carbons, in PCΔ6 the double bonds are shifted three carbons up to the 6th carbon positions, which results in a substantial increase of the main phase transition temperature from -18.3 to 1.0 ^{o}C [86]. When measuring DOPC and PCΔ6 at 10 ^{o}C at which the systems are 28 and 9 ^{o}C above their phase transition temperatures, respectively, one should again expect a substantially faster kinetics in the DOPC membrane. However, the obtained relaxation times τ_r present opposite trends for 10 ^{o}C as well as for 25 ^{o}C. The τ_r decreases from 1.98 ns for DOPC to 1.56 ns for PCΔ6 at 10 ^{o}C and from 1.23 to 1.04 ns at 25 ^{o}C. It is worth noticing that SR kinetics at 10 ^{o}C for PCΔ6 is also much faster than for both POPC and OPPC, even though the T_m of PCΔ6 is the highest. The comparison of SR kinetics in these lipid systems gives clear evidence that the mobility of the hydrated lipid molecules is not only the function of the lipid phase transition temperature. The water molecules bound to the ester-groups probed by Patman are apparently more mobile if the double bonds disturbing lipid packing are located closer to the phospholipid headgroups.

Regarding the level of hydration of the membranes represented by the $\Delta\nu$ parameter we observe a difference at 10 ^{o}C between OPPC and POPC on one side and DOPC and PCΔ6 on the other side. By the level of hydration or the hydration itself we understand here the number of water molecules present in the vicinity of the probe chromophore. In this case, the water molecules are predominantly bound to the lipids. The ester-groups probed by Patman are apparently more hydrated in the case of DOPC and PCΔ6, which possess double unsaturated fatty acid chains. These hydration changes are less detectable at higher temperatures and at 25 ^{o}C they are already within the experimental error (50 cm^{-1}). The $\Delta\nu$ values are in general agreement with SR kinetics (i.e. the larger the $\Delta\nu$ the smaller the τ_r), which means that the increased hydration of the membrane also increases its mobility. The kinetics is, however, much more sensitive to the different lipids.

Summarizing, SR results obtained here for DOPC, POPC, OPPC and PCΔ6 shows that not only the relative temperature to the phase transition temperature influences the mobility in the membrane, but also the position of the double bond in the acyl chain. The closer is the double bond to the sn_1 ester-group, the more mobile this group is.

3.3 SOLVENT RELAXATION IN CATIONIC MEMBRANES

3.3.1 The effect of the surface charge on vesicle size distribution

As it has recently been shown, the curvature of a membrane can affect its hydration properties [44]. Since the surface charge of cationic vesicles may influence both their size and surface properties, the morphology of liposomes should be well characterized after preparation. Dynamic light scattering was used for this purpose. Vesicle suspensions were measured at a right angle. In addition, the radius of gyration was calculated based on light scattering measurements at different angles. When the hydrodynamic radii were compared with the gyration radii, no significant discrepancy was observed for any of the samples used. This justifies the hard sphere model used for fitting the distributions. In addition, vesicle size distributions measured shortly after sample preparation and 5 days later do not show any relevant differences, providing evidence for liposomes stability. The mean radius for all the formulations used was 40 ± 5 nm. All distributions were unimodal with a standard deviation smaller than 15 nm. Taking into account the fact that the mean relaxation times measured by Patman for vesicles with a radius of 10 nm and 100 nm differ by only ~ 25% [44], curvature effects here can be neglected.

3.3.2 Steady-state fluorescence spectra

Excitation and emission spectra of Prodan, Laurdan, and Patman incorporated into LUVs were determined. Representative normalized emission spectra of the three dyes for 0, 50, and 100 mol% of DOTAP in DOPC at 10°C are shown in Figure 3.5. The largest changes were observed for Patman, namely a red-shift occurs and the shoulder on the blue side of the spectrum disappears with increasing DOTAP fraction. These observations may be interpreted in terms of a DOTAP induced relocalization of Patman towards a more polar and/or less viscous microenvironment. The changes in the steady-state spectra are less pronounced for Laurdan, which emission spectrum for liposomes containing 50 mol% of DOTAP is the least red-shifted one.

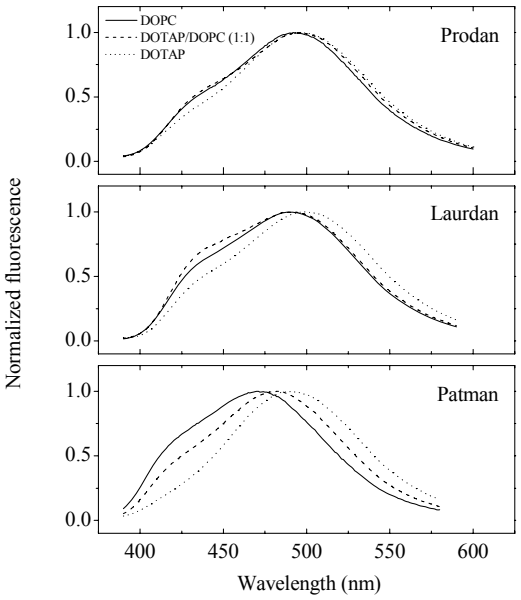

Figure 3.5 Steady-state emission spectra of Prodan, Laurdan, and Patman collected for LUVs formed from DOPC (solid line), DOPC/DOTAP (1:1) (dashed line), and DOTAP (dotted line) at 10 °C. The excitation wavelength was 373 nm.

The spectra of Prodan are not modified by the presence of DOTAP, except for a minute red-shift for liposomes formed from DOTAP alone. It is worth noticing that the spectra of Patman are narrower and less red-shifted than the spectra of the two other dyes. This may indicate that the dye is in a less polar (or more restricted) environment. Such a conclusion is not straightforward, however, since steady-state spectra depend on viscosity as well. In order to weigh the effect of the two processes, an analysis of time-resolved emission spectra is required.

3.3.3 Hydration and mobility of the DOPC/DOTAP liposome membranes

Solvent relaxation measurements were performed for three fluorescent probes: Prodan, Laurdan and Patman embedded into mixed cationic membranes composed of cationic DOTAP and zwitterionic DOPC. Both the lipids contain the same hydrophobic parts consisting of two oleic chains, which assure their low transition temperature. Examples of fluorescence decays of Laurdan in two different formulations are shown in Figure 3.6.

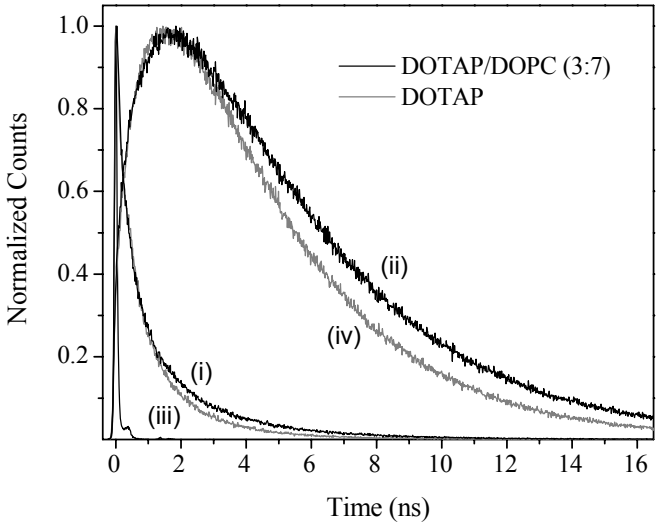

Figure 3.6 Examples of fluorescence decays of Laurdan (λ_{ex} = 373nm) at 10 °C for 30 mol% of DOTAP in DOPC (black lines) at 400nm ((i)) and 540nm ((ii)) and pure DOTAP (grey lines) at 400nm ((iii)) and 540nm ((iv)). Additionally, instrument response function (IRF) is shown.

The TRES reconstructed from the series of fluorescence decays (see Figure 3.7) were fitted using log-normal function, and analyzed in terms of their positions and widths. Examples of TRES position and FWHM cures are given in Figure 3.8. The gradual shift to longer wavelengths and a decrease of the intensity maxima are clearly visible in Figure 3.7. The spectra became wider with time after excitation. The spectral difference between the two samples persists up to the 8th ns. For liposomes formed from pure DOTAP, the spectral shift towards longer wavelengths occurs faster.

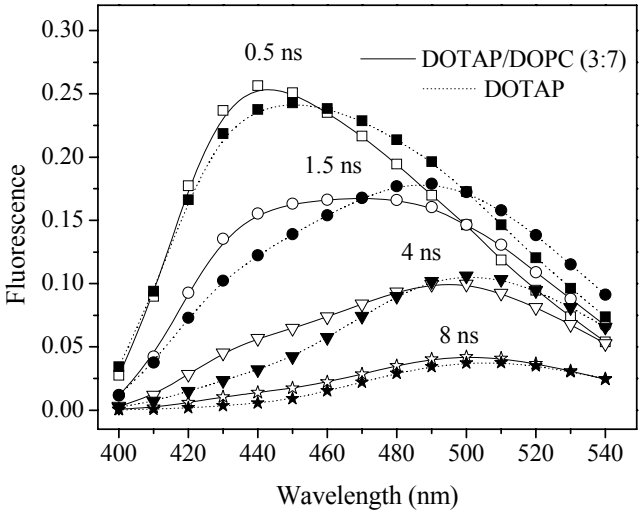

Figure 3.7 Reconstructed time-resolved emission spectra (TRES) for Laurdan at 10 °C for 30 mol% of DOTAP in DOPC (empty symbols and solid lines) and pure DOTAP (filled symbols and dotted lines), at 0.5 ns (squares), 1.5 ns (circles), 4 ns (triangles), and 8 ns (stars) after excitation.

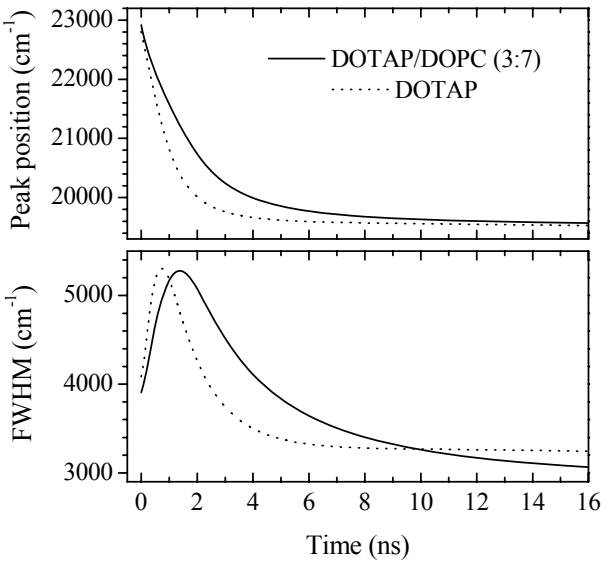

Figure 3.8 The position of the maximum and full width at half maximum (FWHM) of TRES obtained for Laurdan at 10°C for 30 mol % of DOTAP in DOPC (solid lines) and pure DOTAP (dotted lines) as a function of time after excitation.

The Laurdan FWHM profile for liposomes formed from pure DOTAP is shifted to shorter times and larger wavenumbers, which indicates that the environment of Laurdan is more mobile and more heterogeneous, respectively (Figure 3.8). The FWHM profiles for all three dyes in all investigated lipid systems showed clear maxima, providing evidence that solvent relaxation took place within the timescale of the experiment and suggesting a unimodal distribution of the fluorophores. The $\nu(0)$ for the dyes used were estimated to be 23800 cm^{-1}.

Total emission shift, $\Delta\nu$, calculated for Laurdan and Prodan was within the uncertainty of the method (50 cm^{-1}) (Figure 3.9). For Patman, however, an increase of $\Delta\nu$ with increasing DOTAP content is observed. Typically: the larger the $\Delta\nu$ the more hydrated the membrane. The effect was however, larger than any we had previously observed for liquid crystalline membranes. Correct interpretation of the SR results for Patman was possible only after determination of the probes locations within the bilayer (see the previous section). The first part of the $\Delta\nu$ curve of Patman (in the range 0-30 mol% of DOTAP) can be attributed to the fact that the dye is moving outward from the bilayer where it probes more hydrated environment. For the fraction of DOTAP larger than 30 mol% the location of Patman does not change any more (see Table 3.1) thus the continuous increase of $\Delta\nu$ above 30 mol% of DOTAP indicates an increased hydration of the bilayer. This hydration increase is not observed for the two other dyes, which

probe much more hydrated environment already in DOPC bilayer (Figure 3.9). This means that water penetrates deeper into the membrane when the DOTAP content exceeds 30 mol%. Below this value we can only conclude that the hydration at the levels of Laurdan and Prodan does not change significantly.

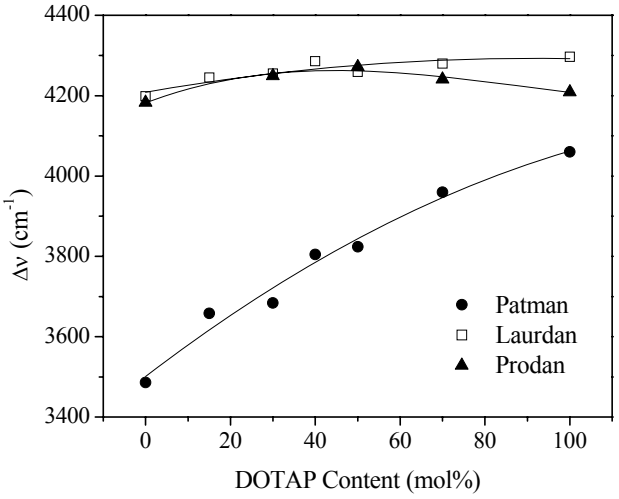

Figure 3.9 Solvent relaxation Δν parameter for Prodan (filled triangles), Laurdan (open squares), and Patman (filled circles) in DOPC/DOTAP LUVs as a function of DOTAP content. Measurements were performed at 10°C. The solid lines are polynomial fits and are shown only as a guide to the eye.

The integrated mean solvent relaxation time (Equation 1.4) is a good measure of relaxation kinetics, provided the spectral response functions do not vary in shape, which was the case in the measured systems. The obtained values of τ_r are plotted in Figure 3.10. Pronounced maxima at around 30 mol% of DOTAP in the lipid bilayer are reported by Laurdan and Prodan. The different behavior of Patman is once again attributed to its relocation. The kinetics of dielectric relaxation in the lipid membrane is often interpreted as the freedom of movement of water hydrating the membrane. At the level where the dyes we use are located water molecules are believed to be fully bound to membrane phospholipids. Therefore, the dynamics of the system as a whole should be considered [43], rather than the slow dynamics of individual water molecules, as it was previously postulated for subnanosecond dynamics observed at protein surfaces [87, 88]. We believe that this is the dynamics of the whole hydrated lipid moieties that we observe and it is better to discuss the results in a general way, referring to bilayer mobility and rigidity [38]. The relaxation time constant depends nonmonotonically on the concentration of cationic lipid. The addition of up to 30 mol% of DOTAP to the DOPC bilayer increases the rigidity of the hydrated functional groups in the vicinity of

the fluorophores of Laurdan and Prodan, which is reflected by the elevated integrated relaxation time.

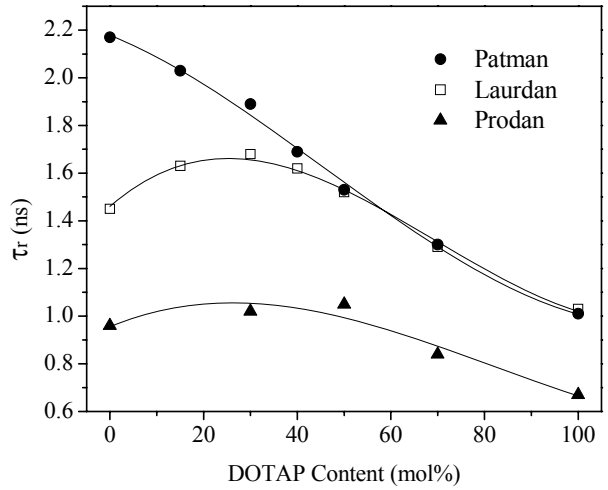

Figure 3.10 Mean solvent relaxation time τ_r (defined by Equation 1.4) for Prodan (filled triangles), Laurdan (open squares), and Patman (filled circles) in DOPC/DOTAP LUVs as a function of DOTAP content. Measurements were performed at 10 °C. The solid lines are best polynomial fits and are shown only as a guide to the eye.

Further addition of DOTAP does not increase τ_r any more, instead the solvation kinetics becomes faster once again, which means that the lipid bilayer is getting more mobile in the closest surrounding of the fluorophores (headgroup region). This nonmnotonic dependence of the membrane headgroup mobility is in good agreement with anomalous mixing of zwitterionic and cationic lipids observed previously in calorimetric studies, where similar maximum was observed in the phase diagram of the mixture of dipalmitoylphosphatidylcholine and cationic dihexadecyldimethylammonium chloride at 35 mol% of cationic compound [89]. It is reasonable that the higher the temperature of the lipid system above its gel-liquid crystalline transition the more mobile the lipid molecules become. Consequently, at the certain temperature, at which all the systems studied are in their liquid crystalline state, the less mobile should be the system, the phase transition temperature of which is the highest. It holds true for our mixtures, which have higher phase transition temperatures than those of the individual pure components. But such relation does not have to be that straight forward and the SR kinetics does not always reflect the temperature offset above the phase transition (see Section 3.2). The reason for the nonideal mixing of zwitterionic and cationic lipids can be a rearrangement of the zwitterionic headgroups as a result of electrostatic interactions

between both the compounds. The phosphatidylcholine headgroup is a dipole, with dipole moment of about 19 D [90], consisting of negatively charged phosphate group and positively charged quaternary ammonium group (in short P-N dipole). It was shown experimentally that in pure phosphatidylcholine bilayer the P-N vector lies almost parallel to the plane of the membrane [91]. Seelig et al., who measured the orientation of the P-N dipole using ^{31}P NMR, observed reorientation of this dipole of more than 30°, when a cationic amphiphile was added [92]. The authors attributed this reorientation to the electrostatic repulsion between the cationic headgroup and the N^+ end of the P-N dipole (see Figure 3.1). More recent molecular dynamics simulations of the mixture of dimyristoylphosphatidylcholine (DMPC) and dimyristoyltrimethylammoniumpropane (DMTAP) showed the increase of the angle between the P-N dipole of DMPC and bilayer surface from 10° in pure DMPC to 60° in 50 mol% and more of DMTAP [93]. This reorientation resulted in decreased area per lipid for the DMPC/DMTAP (1:1) mixture. Above 50 mol% of DMTAP the bilayer expanses again due to repulsion between the cationic headgroups. The curve of the area per lipid as a function of DMTAP content [93] was very simmilar to the τ_r curve we obtained for Laurdan (Figure 3.8); except the maximum, in our case, is at 30 mol% of the cationic lipid. To our best knowledge our SR measurements gave the first experimental confirmation of these nonmonotonic changes in lipid packing in fully hydrated free standing mixed cationic membranes (Figure 3.11). The discrepancy between the positions of the maxima can be the effect of different backbones of the lipids used (oleic versus myristic chains). This hypothesis motivated the SR studies on DMPC/DMTAP system.

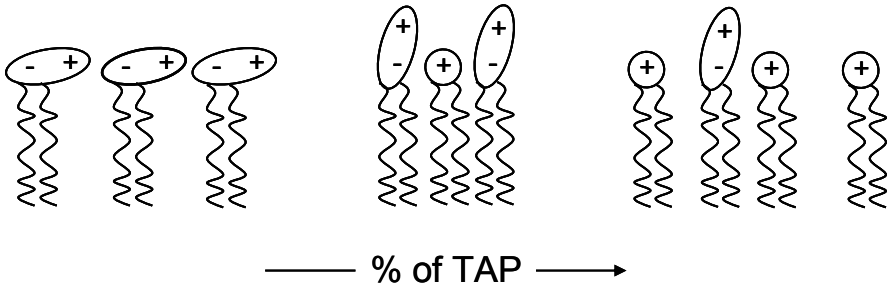

Figure 3.11 Scheme presenting headgroup rearrangement in mixtures of cationic and zwitterionic lipids

3.3.4 DMPC/DMTAP versus DOPC/DOTAP

SR measurements analogous to the presented above were performed for DMPC/DMTAP system, to study the influence of the hydrocarbon chains on the mobility and hydration of the headgroup region of these mixed cationic membranes. The myristic chains are shorter than the oleic ones and fully saturated. To compare both systems only Laurdan data, for which the changes were the most pronounced, was used. The DMPC/DMTAP membranes were measured at 50 °C to keep approximately the same temperature offset above the main phase transition temperatures of both the systems. The $\Delta\nu$ and τ_r parameters are presented in Figure 3.12 and Figure 3.13, respectively; the results obtained previously for DOPC/DOTAP membrane are included for comparison.

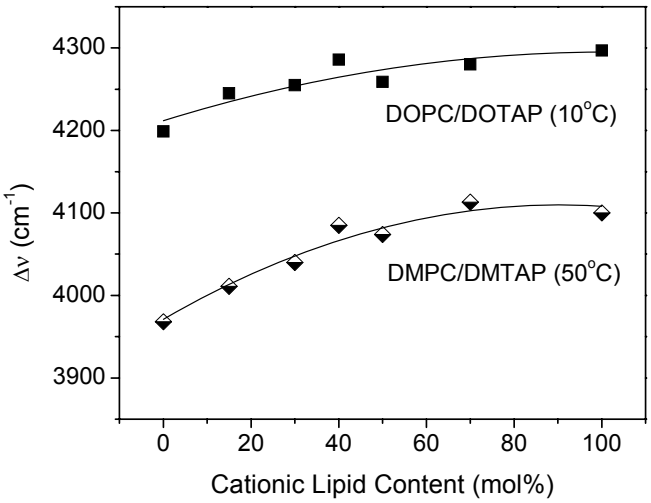

Figure 3.12 Solvent relaxation $\Delta\nu$ parameter for Laurdan in DOPC/DOTAP LUVs (squares) and DMPC/DMTAP LUVs (diamonds) as a function of cationic lipid content. Measurements were performed at 10 °C and 50 °C for DOPC/DOTAP and DMPC/DMTAP systems, respectively. The best polynomial fits (solid lines) are shown for eye guidance.

The increase of $\Delta\nu$ values with increasing TAP content was more pronounced for the DMPC/DMTAP system (Figure 3.12). Although, the overall change in DMPC/DMTAP hydration was not large, the bilayer hydrated gradually when percentage of DMTAP increased. The higher hydration of DOPC than DMPC is not a surprise as the double unsaturated backbones of DOPC create molecule with bulkier backbone, hence, the

larger area per lipid leaves more space for water at the headgroup region; in comparison with DMPC with saturated myristic chains.

The maximum of mean relaxation time is also present for DMPC/DMTAP membrane, although it is shifted to 45 mol% of DMTAP content (Figure 3.13). This discrepancy is a straight forward consequence of the different geometries of DMPC and DOPC molecules. The membrane area per DMPC molecule is smaller and more dependent on its headgroup than on its hydrophobic part.

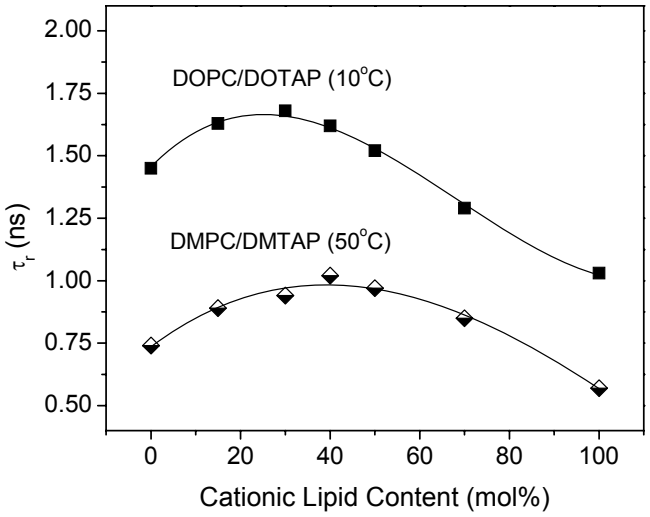

Figure 3.13 Mean solvent relaxation time τ_r (defined by Equation 1.4) for Laurdan in DOPC/DOTAP LUVs (squares) and DMPC/DMTAP LUVs (diamonds) as a function of cationic lipid content. Measurements were performed at 10 °C and 50 °C for DOPC/DOTAP and DMPC/DMTAP bilayers, respectively. The best polynomial fits (solid lines) are shown for eye guidance.

When the P-N dipoles raise, the DMPC bilayer compresses considerably, while the DOPC compressibility is restricted by its bulky hydrophobic part and finishes at lower cationic lipid content. It is worth noticing that the relative changes in the relaxation time are considerably bigger for DMPC/DMTAP bilayer (Figure 3.13), i.e. τ_r at 45 mol% of DMTAP is 30 % longer than for pure DMPC, while τ_r at 30 mol% of DOTAP is only 15 % longer than the one for pure DOPC. The results obtained for DMPC/DMTAP membrane are in very good agreement with the previously mentioned molecular simulations of the same system, where the maximum compression was achieved at around 50 mol% of DMTAP [93]. It was shown that in some cationic membranes at high cationic lipid content the expansion of the membrane can cause the interdigitation of the bilayer leaflets [94]. In both the systems presented here no signs of interdigitation were observed.

4 CONCLUSIONS

Solvent relaxation method based on time-resolved measurements of fluorescent probes with defined locations within the lipid bilayer is a valuable tool, suitable for monitoring the hydration and organization of fully hydrated biological and model membranes. The goal of this doctoral thesis was: 1) find the precise location of fluorescent headgroup probes within the model lipid membranes; 2) characterize the solvation dynamics of different neutral lipid bilayer compositions which could help better understand the fluorescence solvent relaxation process on the molecular level; 3) using fluorescence solvent relaxation method characterize dynamics of cationic membranes, structures more and more popular in gene therapy. The most important results are put together below:

- The solvation dynamics in the headgroup region which was monitored along the normal plane of the phospholipid bilayers seems to be purely nanosecond excluding the presence of the so-called "bulk" water. Decrease of the hydration and mobility was observed when moving toward the centre of the bilayer.

- When a set of dyes that share the same chromophore, but differ in their location within the bilayer is applied, it allows compare hydration and mobility of lipid bilayer at different depths inside the membrane. In order to determine the precise location of two headgroup fluorescent probes (Laurdan and Patman), parallax quenching method was used.

- Parallax quenching results shows that even thought the distance between two particular dyes probing the headgroup region of the lipid membrane is very small (~ 1 Å), the huge polarity gradient present in this region significantly influences solvent relaxation results.

- Quenching with acrylamide provided a simple and reliable test for potential dye relocation.

- Quenching experiments with acrylamide showed that only neutral probe (e.g. Laurdan) is acceptable for positively charged membrane measurements. Selection of the charged probe (e.g. Patman) can result in the misinterpretation of the solvent relaxation results.

- Solvent relaxation measurements shows that differences in mobility at the glycerol level can be observed for the PC bilayers with different hydrocarbon tails. A very strong dependence of SR kinetics on the position of double bond in the fatty acid chains was observed which proves that SR approach can report mobility changes within phospholipid bilayers with a remarkable molecular resolution.

- The SR properties of DOPC/DOTAP cationic membranes were investigated. The observed nonmonotonic dependence of relaxation properties on DOTAP content in the DOPC bilayer supports a scenario of headgroup rearrangement in mixtures of cationic and zwitterionic lipids [92-95]. This finding may have important implications for the development of synthetic genetic information carriers, e.g. it correlates with the interaction profile of cationic vesicles with oligonucleotides, for which maximum association was found at ~25 % of DOTAP [96].

- In order to investigate how does the change of the hydrophobic part of the lipid membrane (i.e. different alkyl chains) influences bilayer structure, measurements with the DMPC/DMTAP liposomes were performed.

- Comparing both the above systems, i.e. DOPC/DOTAP versus DMPC/DMTAP, the influence of the different alkyl chains was clearly seen, i.e. the smallest area per lipid was observed at different cationic lipid content in the lipid membrane (at 30 mol% in the case of the DOPC/DOTAP system and ~45 mol% in the case of the other one).

ACNOWLEDGEMENTS

First of all I want to thank my supervisor, Martin Hof. Martin, I am grateful for giving me the opportunity to work in your group. Your patience and friendly attitude cause that I have never regret coming to Prague.

During all these years I have had a great pleasure to share the room at work with two great people, Teresa & Piotr. Tereso, thank you for endless discussions on so many subjects we had at work and off work, for quarrels;) and trips we had together finished with: "So, back again", and … many, many other things. Piotr, thank you for introducing me into solvent relaxation topic, for all "annoying" question concerning the SR method you had always prepared for me;), and willingness to help and discuss science at any time for all this years. Thanks for all summer and winter mountain "adventures":]. And at last let me thank you for reading this manuscript and your comments.

My deep gratitude goes also to another "SR man", Jan Sýkora. Honzo, I believe you can find answer for almost every scientific, and not only, question:). And yours "Oh, no!" and "with pleasure" I will always remember:).

I thank other members of our group: Justyna Barucha, Aleš Benda, Lenka Beranová, Basia Gasińska, Jana Humpoličkova, Radek Machaň, Adam Miszta, Radek Šahl, Martin Štefl and Ania Zań. I really appreciate relax working atmosphere we managed to create together, which was only occasionally disturbed by small "storms";)

I must express my gratitude to Karel Procházka for the access to the dynamic light scattering instrumentation and Mirek Štěpánek for his help.

I am grateful my "old" colleagues and friends as well as people who I have met during these last four years: Magda Przybyło, Tomek Borowik, Agnieszka & Piotr Żukowski, Dorota Szczęsna, Agnieszka i Damian Bajrakowie, Ivan Jirka, Kaska Janik, Tomek Radlak, Rafal & Ania Hrynyk, Justyna Pawlesa, Eva Grigorova and others:). You have been making my everyday live more interesting and colorful.

I owe a lot of appreciation to the administrative staff of the JH Institute and, particularly, our secretary Mrs. Vladimíra Bergerová for their willingness to help with bureaucratic, and not only, problems.

Finally, I must express my gratefulness to my family; my aunt and uncle, Irena & Wiesław Janik, who are always ready to help me; my brother, Piotr, for his patience for hot-tempered younger sister;); and at last but not least, to my mother, Hanna, for her love, trust and freedom she has given me.

In the very end I wish to express my gratitude for financial support to: Heyrovský Institute of Physical Chemistry and Grant Agency of the Academy of Sciences of the Czech Republic (via 203/05/H001).

REFERENCES

1. P. C. Nelson, *Physic Inside The Cell*. (2002).

2. G. Gregoriadis, Engineering Liposomes for Drug Delivery: Progress and Problems, *Trends Biotechnol.* (1995) **13**(12): 527-537.

3. M. Langner, and T. E. Kral, Liposome-Based Drug Delivery Systems, *Polish J. Pharmac.* (1999) **51**(3): 211-222.

4. M. C. Woodle, and D. D. Lasic, Sterically Stabilized Liposomes, *Biochim. Biophys. Acta* (1992) **1113**(2): 171-199.

5. P. V. Escriba, Membrane-Lipid Therapy: A New Approach in Molecular Medicine, *Trends Mol. Med.* (2006) **12**(1): 34-43.

6. J. M. Seddon, Lyotropic Phase Behaviour of Biological Amphiphiles, *Berichte Der Bunsen-Gesellschaft - Phys. Chem. Chem. Phys.* (1996) **100**(3): 380-393.

7. J. N. Israelachvili, S. Marcelja, and R. G. Horn, Physical principles of membrane organization, *Q. Rev. Biophys.* (1980) **13**: 121-200.

8. J. M. Seddon, Structure of the Inverted Hexagonal (H_{II}) Phase, and Non-Lamellar Phase-Transitions of Lipids, *Biochim. Biophys. Acta* (1990) **1031**(1): 1-69.

9. B. Albert, D. Bray, J. Lewis, M. Raff, K. Roberts, and J. D. Watson, *Molecular Biology of the Cell*. (Garland, New York, 1989).

10. A. D. Bangham, M. M. Standish, and J. C. Watkins, Diffusion of univalent ions across the lamellae of swollen phospholipids, *J. Mol. Biol.* (1965) **13**: 238-252.

11. M. J. Hope, M. B. Bally, L. D. Mayer, A. S. Janoff, and P. R. Cullis, Generation of Multilamellar and Unilamellar Phospholipid-Vesicles, *Chem. Phys. Lipids* (1986) **40**(2-4): 89-107.

12. L. A. Bagatolli, Direct observation of lipid domains in free standing bilayers: from simple to complex lipid mixtures, (2003) **122**(1-2): 137-145.

13. L. A. Bagatolli, To see or not to see: Lateral organization of biological membranes and fluorescence microscopy, (2006) **1758**(10): 1541-1556.

14. S. Costigan, P. J. Booth, and R. H. Templer, *Biochim. Biophys. Acta* (2000) **1468**: 41-54.

15. J. F. Nagle, and S. Tristram-Nagle, Structure of lipid bilayers, *Biochim. Biophys. Acta* (2000) **1469**: 159-195.

16. S. J. Marrink, and H. J. C. Berendsen, Simulation of Water Transport through a Lipid-Membrane, *J. Phys. Chem.* (1994) **98**(15): 4155-4168.

17. R. F. Epand, R. Kraayenhof, G. J. Sterk, H. W. W. F. Sang, and R. M. Epand, Flourescent probes of membrane surface properties, *Biochim. Biophys. Acta* (1996) **1284**: 191-195.

18. R. D. Kaiser, and E. London, Location of diphenylhexatriene (DPH) and its derivatives within membranes: comparition of different fluorescence quenching analysis of membrane depth, *Biochemistry* (1998) **37**: 8180-8190.

19. S. H. White, and M. C. Wiener, Determination of the structure of fluid lipid bilayer membranes. In *Permeability and stability of lipid bilayers*, edited by E. A. Disalvo and S. A. Simon, (CRC Press, Boca Raton, 1995), pp. 1-19.

20. S. J. Marrink, and A. E. Mark, Effect of undulations on surface tension in simulated bilayers, *J. Phys. Chem. B* (2001) **105**: 6122-6127.

21. S. J. Marrink, D. P. Tieleman, A. R. v. Buuren, and H. J. C. Berendsen, Membrane and water: an interesting relationship, *Faraday Discuss.* (1996) **103**: 191-201.

22. S. J. Eastman, C. Siegel, J. Tousignant, A. E. Smith, S. H. Cheng, and R. K. Scheule, Biophysical characterization of cationic lipid:DNA complexes, *Biochim. Biophys. Acta* (1997) **1325**: 41-62.

23. M. Langner, The intracellular fate of non-viral DNA carriers, *Cell. Molec. Biol. Lett.* (2000) **5**: 295-313.

24. J. Gabrielska, S. Przestalski, A. Miszta, M. Soczynska-Kordala, and M. Langner, The effect of cholesterol on the absorption of phenyltin compounds onto phosphatidylcholine and sphingomyelin liposome membranes, *Appl. Organomet. Chem.* (2004) **18**: 9-14.

25. R. Hutterer, F. W. Schneider, W. T. Hermens, R. Wagenvoord, and M. Hof, Binding of prothrombin and its fragment 1 to phospholipid membranes studied by the solvent relaxation technique, *Biochim. Biophys. Acta* (1998) **1414**(1-2): 155-164.

26. R. Hutterer, F. W. Schneider, and M. Hof, Time-Resolved Emission Spectra and Anisotropy Profiles for Symmetric Diacyl- and Dietherphosphatidylcholines, *J. Fluorescence* (1997) **7**: 27-33.

27. A. S. Klymchenko, G. Duportail, A. P. Demchenko, and Y. Mely, Bimodal distribution and fluorescence response of environment-sensitive probes in lipid bilayers, *Biophys. J.* (2004) **86**(5): 2929-2941.

28. M. Langner, and H. Kleszczynska, Estimation of the organic compounds partition into phosphatidylcholine bilayers with pH sensitive fluorescence probe, *Cell. Mol. Biol. Lett.* (1997) **2**: 15-24.

29. A. Olzynska, M. Przybylo, J. Gabrielska, Z. Trela, S. Przestalski, and M. Langner, Di- and tri-phenyltin chlorides transfer across a model lipid bilayer, *Appl. Organomet. Chem.* (2005) **19**(10): 1073-1078.

30. P. Jurkiewicz, J. Sykora, A. Olzynska, J. Humplickova, and M. Hof, Solvent relaxation in phospholipid bilayers: Principles and recent applications, *J. Fluorescence* (2005) **15**(6): 883-894.

31. E. G. Finer, and A. Darke, Phospholipid Hydration Studied by Deuteron Magnetic-Resonance Spectroscopy, *Chem. Phys. Lipids* (1974) **12**(1): 1-16.

32. P. O. Westlund, Line shape analysis of NMR powder spectra of (H2O)-H-2 in lipid bilayer systems, *J. Phys. Chem. B* (2000) **104**(25): 6059-6064.

33. D. L. Bernik, D. Zubiri, E. Tymczyszyn, and E. A. Disalvo, Polarity and packing at the carbonyl and phosphate regions of lipid bilayers, *Langmuir* (2001) **17**(21): 6438-6442.

34. S. Mazeres, V. Schram, J. F. Tocanne, and A. Lopez, 7-nitrobenz-2-oxa-1,3-diazole-4-yl-labeled phospholipids in lipid membranes: Differences in fluorescence behavior, *Biophys. J.* (1996) **71**(1): 327-335.

35. M. C. Rheinstadter, C. Ollinger, G. Fragneto, F. Demmel, and T. Salditt, Collective dynamics of lipid membranes studied by inelastic neutron scattering, *Phys. Rev. Lett.* (2004) **93**(10):

36. S. Tristram-Nagle, and J. F. Nagle, Lipid bilayers: thermodynamics, structure, fluctuations, and interactions, *Chem. Phys. Lipids* (2004) **127**(1): 3-14.

37. R. Hutterer, A. B. J. Parusel, and M. Hof, Solvent relaxation of Prodan and Patman: A useful tool for the determination of polarity and rigidity changes in membranes, *J. Fluorescence* (1998) **8**(4): 389-393.

38. R. Hutterer, F. W. Schneider, H. Sprinz, and M. Hof, Binding and relaxation behaviour of Prodan and Patman in phospholipid vesicles: A fluorescence and H-1 NMR study, *Biophys. Chem.* (1996) **61**(2-3): 151-160.

39. J. Sykora, and M. Hof, Solvent relaxation in phospholipid bilayers: Physical understanding and biophysical applications, *Cell. Mol. Biol. Lett.* (2002) **7**(2): 259-261.

40. R. S. Fee, and M. Maroncelli, Estimating the Time-Zero Spectrum in Time-Resolved Emission Measurements of Solvation Dynamics, *Chem. Phys.* (1994) **183**(2-3): 235-247.

41. M. L. Horng, J. A. Gardecki, A. Papazyan, and M. Maroncelli, Subpicosecond Measurements of Polar Solvation Dynamics - Coumarin-153 Revisited, *J. Phys. Chem.* (1995) **99**(48): 17311-17337.

42. J. Sykora, P. Kapusta, V. Fidler, and M. Hof, On what time scale does solvent relaxation in phospholipid bilayers happen?, *Langmuir* (2002) **18**(3): 571-574.

43. L. Nilsson, and B. Halle, Molecular origin of time-dependent fluorescence shifts in proteins, *Proc. Natl. Acad. Sci. USA* (2005) **102**(39): 13867-13872.

44. J. Sykora, P. Jurkiewicz, R. M. Epand, R. Kraayenhof, M. Langner, and M. Hof, Influence of the curvature on the water structure in the headgroup region of phospholipid bilayer studied by the solvent relaxation technique, *Chem. Phys. Lipids* (2005) **135**(2): 213-221.

45. M. Hof, *Solvent Relaxation in Biomembranes*. (Springer Verlag, Berlin, 1999), p 439-456.

46. J. Sykora, V. Mudogo, R. Hutterer, M. Nepras, J. Vanerka, P. Kapusta, V. Fidler, and M. Hof, ABA-C-15: A new dye for probing solvent relaxation in phospholipid bilayers, *Langmuir* (2002) **18**(24): 9276-9282.

47. M. Yang, and R. Richert, Observation of heterogeneity in the nanosecond dynamics of a liquid, *J. Chem. Phys.* (2001) **115**(6): 2676-2680.

48. R. Richert, Spectral diffusion in liquids with fluctuating solvent responses: Dynamical heterogeneity and rate exchange, *J. Chem. Phys.* (2001) **115**(3): 1429-1434.

49. P. Dutta, P. Sen, S. Mukherjee, A. Halder, and K. Bhattacharyya, Solvation dynamics in the water pool of an aerosol-OT microemulsion. Effect of sodium salicylate and sodium cholate, *J. Phys. Chem. B* (2003) **107**(39): 10815-10822.

50. J. Faeder, and B. M. Ladanyi, Solvation dynamics in reverse micelles: The role of headgroup-solute interactions, *J. Phys. Chem. B* (2005) **109**(14): 6732-6740.

51. R. Jimenez, G. R. Fleming, P. V. Kumar, and M. Maroncelli, Femtosecond Solvation Dynamics of Water, *Nature* (1994) **369**(6480): 471-473.

52. G. Weber, and F. J. Farris, Synthesis and Spectral Properties of a Hydrophobic Fluorescent-Probe - 6-Propionyl-2-(Dimethylamino)Naphthalene, *Biochemistry* (1979) **18**(14): 3075-3078.

53. P. L. G. Chong, Effects of Hydrostatic-Pressure on the Location of Prodan in Lipid Bilayers and Cellular Membranes, *Biochemistry* (1988) **27**(1): 399-404.

54. R. Hutterer, and M. Hof, Probing ethanol-induced phospholipid phase transitions by the polarity sensitive fluorescence probes Prodan and Patman, *Z. Phys. Chem.* (2002) **216**: 333-346.

55. K. Rieber, J. Sykora, A. Olzynska, R. Jelinek, G. Cevc, and M. Hof, The use of solvent relaxation technique to investigate headgroup hydration and protein binding of simple and mixed phosphatidylcholine/surfactant bilayer membranes, *Biochim. Biophys. Acta* (2007) **1768**(5): 1050-1058.

56. T. Parasassi, E. K. Krasnowska, L. Bagatolli, and E. Gratton, LAURDAN and PRODAN as polarity-sensitive fluorescent membrane probes, *J. Fluorescence* (1998) **8**(4): 365-373.

57. P. L. G. Chong, and P. T. T. Wong, Interactions of Laurdan with Phosphatidylcholine Liposomes - a High-Pressure Ftir Study, *Biochim. Biophys. Acta* (1993) **1149**(2): 260-266.

58. M. Viard, J. Gallay, M. Vincent, and M. Paternostre, Origin of laurdan sensitivity to the vesicle-to-micelle transition of phospholipid-octylglucoside system: A time-resolved fluorescence study, *Biophys. J.* (2001) **80**(1): 347-359.

59. J. R. Lakowicz, D. R. Bevan, B. P. Maliwal, H. Cherek, and A. Balter, Synthesis and Characterization of a Fluorescence Probe of the Phase-Transition and Dynamic Properties of Membranes, *Biochemistry* (1983) **22**(25): 5714-5722.

60. S. W. Hui, M. Langner, Y. L. Zhao, P. Ross, E. Hurley, and K. Chan, The role of helper lipids in cationic liposome-mediated gene transfer, *Biophys. J.* (1996) **71**: 590-599.

61. T. Kral, A. Benda, M. Hof, and M. Langner, Some aspects of DNA condensation observed by fluorescence correlation spectroscopy. In *Rev. Fluorescence*, edited by C. D. Geddes and J. R. Lakowicz, (Springer, New York, 2005), pp. 109-124.

62. T. Kral, M. Hof, P. Jurkiewicz, and M. Langner, Fluorescence correlation spectroscopy (FCS) as a tool to study DNA condensation with hexadecyltrimethylammonium bromide (HTAB), *Cell. Mol. Biol. Lett.* (2002) **7**: 203-211.

63. J. O. Radler, I. Koltover, T. Salditt, and C. R. Safinya, Structure of DNA-cationic liposome complexes: DNA intercalation in multilamellar membranes in distinct interhelical packing regimes, *Science* (1997) **275**(5301): 810-814.

64. P. L. Felgner, T. R. Gadek, M. Holm, R. Roman, H. W. Chan, M. Wenz, J. P. Northrop, G. M. Ringold, and M. Danielsen, Lipofection - a Highly Efficient, Lipid-Mediated DNA-Transfection Procedure, *Proc. Natl. Acad. Sci. U. S. A.* (1987) **84**(21): 7413-7417.

65. M. Langner, and K. Kubica, The electrostatics of lipid surfaces, *Chem. Phys. Lipids* (1999) **101**(1): 3-35.

66. G. Byk, J. Sato, C. Mattler, M. Frederic, and D. Scherman, Novel non-viral vector for gene delivery: synthesis of a second-generation library of mono-functionalized poly-(guanidinium)amines and their introduction into cationic lipids, *Biotech. Bioeng.* (1998) **61**: 81-87.

67. G. Byk, and D. Scherman, Novel cationic lipids for gene delivery and gene therapy, *Exp. Opin. Ther. Patents* (1998) **8**: 1125-1141.

68. T. Borowik, K. Widerak, M. Ugorski, and M. Langer, Combined effect of surface electrostatic charge and poly(ethyl glycol) on the association of liposomes with colon carcinoma cells, *J. Liposome Res.* (2005) **15**(3-4): 199-213.

69. K. L. Hong, W. W. Zheng, A. Baker, and D. Papahadjopoulos, Stabilization of cationic liposome-plasmid DNA complexes by polyamines and poly(ethylene glycol)-phospholipid conjugates for efficient in vivo gene delivery, *FEBS Lett.* (1997) **400**(2): 233-237.

70. A. Martin-Herranz, A. Ahmad, H. M. Evans, K. Ewert, U. Schulze, and C. R. Safinya, Surface functionalized cationic lipid-DNA complexes for gene delivery: PEGylated lamellar complexes exhibit distinct DNA-DNA interaction regimes, *Biophys. J.* (2004) **86**(2): 1160-1168.

71. L. Stamatatos, R. Leventis, M. J. Zuckermann, and J. R. Silvius, Interactions of Cationic Lipid Vesicles with Negatively Charged Phospholipid-Vesicles and Biological-Membranes, *Biochemistry* (1988) **27**(11): 3917-3925.

72. D. Hirsch-Lerner, and Y. Barenholz, Probing DNA-cationic lipid interactions with the fluorophore trimethylammonium diphenyl-hexatriene (TMADPH), *Biochim. Biophys. Acta* (1998) **1370**(1): 17-30.

73. K. Lenssen, P. Jantscheff, G. von Kiedrowsld, and U. Massing, Combinatorial synthesis of new cationic lipids and high-throughput screening of their transfection properties, *ChemBioChem* (2002) **3**: 852-858.

74. Y. K. Ghosh, S. S. Visweswariah, and S. Bhattacharya, Advantage of the ether linkage between the positive charge and the cholesterol-based amphiphiles as vectors for gene delivery, *Bioconjug. Chem.* (2002) **13**: 378-384.

75. R. Leventis, and J. R. Silvius, Interactions of mammalian cells with lipid dispersions containing novel metabolizable cationic amphiphiles, *Biochim. Biophys. Acta* (1990) **1023**: 124-132.

76. N. J. Zuidam, and Y. Barenholtz, Electrostatic parameters of cationic liposomes commonly used for gene delivery as determined by 4-heptadecyl-7-hydroxycoumarin, *Biochim. Biophys. Acta* (1997) **1329**: 211-222.

77. D. Simberg, D. Hirsch-Lerner, R. Nissim, and Y. Barenholz, Comparison of different commercially available cationic lipid-based transfection kits, *J. Liposome Res.* (2000) **10**: 1-13.

78. J. R. Lakowicz, *Principles of Fluorescence Spectroscopy*. (Kluwer-Plenum Press, New York, NY, 1999).

79. A. Chattopadhyay, and E. London, Parallax Method for Direct Measurement of Membrane Penetration Depth Utilizing Fluorescence Quenching by Spin-Labeled Phospholipids, *Biochemistry* (1987) **26**(1): 39-45.

80. F. S. Abrams, and E. London, Extension of the Parallax Analysis of Membrane Penetration Depth to the Polar-Region of Model Membranes - Use of Fluorescence Quenching by a Spin-Label Attached to the Phospholipid Polar Headgroup, *Biochemistry* (1993) **32**(40): 10826-10831.

81. P. E. G. Thoren, D. Persson, E. K. Esbjorner, M. Goksor, P. Lincoln, and B. Norden, Membrane binding and translocation of cell-penetrating peptides, *Biochemistry* (2004) **43**(12): 3471-3489.

82. D. E. Koppel, Analysis of Macromolecular Polydispersity in Intensity Correlation Spectroscopy - Method of Cumulants, *J. Chem. Phys.* (1972) **57**(11): 4814-&.

83. S. W. Provencher, A Constrained Regularization Method for Inverting Data Represented by Linear Algebraic or Integral-Equations, *Comput. Phys. Commun.* (1982) **27**(3): 213-227.

84. S. S. Antollini, and F. J. Barrantes, Disclosure of discrete sites for phospholipid and sterols at the protein-lipid interface in native acetylcholine receptor-rich membrane, *Biochemistry* (1998) **37**(47): 16653-16662.

85. C. D. Geddes, Optical halide sensing using fluorescence quenching: theory, simulations and applications - a review, *Meas. Sci. Technol.* (2001) **12**(9): R53-R88.

86. R. Koynova, and M. Caffrey, Phases and phase transitions of the phosphatidylcholines, *Biochim. Biophys. Acta-Rev. Biomem.* (1998) **1376**(1): 91-145.

87. K. Bhattacharyya, and B. Bagchi, Slow dynamics of constrained water in complex geometries, *J. Phys. Chem. A* (2000) **104**(46): 10603-10613.

88. S. K. Pal, and A. H. Zewail, Dynamics of water in biological recognition, *Chem. Rev.* (2004) **104**(4): 2099-2123.

89. J. R. Silvius, Anomalous Mixing of Zwitterionic and Anionic Phospholipids with Double-Chain Cationic Amphiphiles in Lipid Bilayers, *Biochim. Biophys. Acta* (1991) **1070**(1): 51-59.

90. J. C. W. Shepherd, and G. Buldt, Zwitterionic dipoles as a dielectric probe for investigating head group mobility in phospholipid membranes, *Biochim. Biophys. Acta* (1978) **514**(1): 83-94.

91. J. Seelig, P. M. Macdonald, and P. G. Scherer, Phospholipid head groups as sensors of electric charge in membranes, *Biochemistry* (1987) **26**(24): 7535-7541.

92. P. G. Scherer, and J. Seelig, Electric Charge Effects on Phospholipid Headgroups - Phosphatidylcholine in Mixtures with Cationic and Anionic Amphiphiles, *Biochemistry* (1989) **28**(19): 7720-7728.

93. A. A. Gurtovenko, M. Patra, M. Karttunen, and I. Vattulainen, Cationic DMPC/DMTAP lipid bilayers: Molecular dynamics study, *Biophys. J.* (2004) **86**(6): 3461-3472.

94. S. J. Ryhanen, J. M. I. Alakoskela, and P. K. J. Kinnunen, Increasing surface charge density induces interdigitation in vesicles of cationic amphiphile and phosphatidylcholine, *Langmuir* (2005) **21**(13): 5707-5715.

95. L. F. Zhang, T. A. Spurlin, A. A. Gewirth, and S. Granick, Electrostatic stitching in gel-phase supported phospholipid bilayers, *J. Phys. Chem. B* (2006) **110**(1): 33-35.

96. P. Jurkiewicz, A. Okruszek, M. Hof, and M. Langner, Associating oligonucleotides with positively charged liposomes, *Cell. Molec. Biol. Lett.* (2003) **8**: 77-84.